

Global change factors influence different aspects of arbuscular mycorrhizal fungal communities

Junqiang Zheng (✉ zhjq79@yahoo.com)

Henan University <https://orcid.org/0000-0003-0129-690X>

Mingming Cui

Henan University

Cong Wang

Henan University College of Life Science

Jian Wang

Henan University College of Life Science

Shilin Wang

Henan University College of Life Science

Zhongjie Sun

Henan University College of Life Science

Feirong Ren

Henan University College of Life Science

Shiqiang Wan

Hebei University College of Life Sciences

Shijie Han

Henan University College of Life Science

Research

Keywords: Nitrogen deposition, Global change, Arbuscular mycorrhizal fungi, Grassland, Semiarid ecosystem, Elevated CO₂, Increased precipitation

Posted Date: February 25th, 2021

DOI: <https://doi.org/10.21203/rs.3.rs-243669/v1>

License:  This work is licensed under a Creative Commons Attribution 4.0 International License.

[Read Full License](#)

Global change factors influence different aspects of arbuscular mycorrhizal fungal communities

Junqiang Zheng^{1,2}, Mingming Cui^{1,2}, Cong Wang^{1,2}, Jian Wang^{1,2}, Shilin Wang^{1,2}, Zhongjie Sun^{1,2}, Feirong Ren^{1,2}, Shiqiang Wan³, Shijie Han^{1,2}

1 International Joint Research Laboratory for Global Change Ecology, School of Life Sciences, Henan University, Kaifeng, 475004, Henan, China

2 Yellow River Floodplain Ecosystems Research Station, Henan University, Xinyang, China

3 College of Life Sciences, Institute of Life Science and Green Development, Hebei University, Baoding, 071002, Hebei, China

Correspondence

Shijie Han and Junqiang Zheng, Room 623, School of Life Sciences, Henan University, Kaifeng, Henan 475004, China.

Email: zhjq79@yahoo.com (J. Q. Z) and Email: hansj@iae.ac.cn (S. J. H)

Abstract:

Background

The functional diversity of arbuscular mycorrhizal fungi (AMF) affects the resistance and resilience of plant communities to environmental stresses. However, considerable uncertainty remains about how the complex interactions among elevated atmospheric CO₂ (eCO₂), nitrogen deposition (eN), increased precipitation (eP), and warming (eT) affect AMF communities. These global change factors (GCFs) always occur simultaneously, and their interactions likely affect AMF community structure and assembly processes. In this study, the interactive effects of these four GCFs on AMF communities were explored in an open-top chamber field experiment in a semiarid grassland.

Results

Elevated CO₂, eN, eT, and eP and their interactions did not affect AM fungal biomass. The relative abundance of *Paraglomus* increased with N addition across treatment combinations, whereas that of *Glomus* decreased with N addition, especially combined with eT and eCO₂. Precipitation, T, and N affected AMF phylogenetic α -diversity, and the three-way interaction among CO₂, T, and N affected taxonomic and phylogenetic α -diversity. Nitrogen addition significantly affected the β -diversity of AMF communities. Both variable selection and dispersal limitation played major roles in shaping AMF communities, whereas homogeneous selection and homogenizing dispersal had almost no influence on AMF community assembly. The contribution of variable selection decreased under eCO₂, eN and eT, but not under eP. The contribution of dispersal limitation decreased under eCO₂, eT, and eP but it increased under eN. The assembly of AMF communities under the sixteen GCF combinations was strongly influenced by dispersal limitation, variable selection and ecological drift.

Conclusions

Elevated CO₂, warming, N addition, and increased precipitation influenced different aspects of AMF communities. The interactive effects of the four GCFs on AMF communities were limited. Collectively, the results of this study suggest that AMF communities in semiarid grasslands can resist changes in the global climate.

Keywords: Nitrogen deposition; Global change; Arbuscular mycorrhizal fungi; Grassland; Semiarid ecosystem; Elevated CO₂; Increased precipitation

Background

Global atmospheric carbon dioxide (CO₂) concentrations and nitrogen (N) deposition have steadily increased since 1850 from 280 ppm and 23 Tg N yr⁻¹ to over 400 ppm and 132 Tg N yr⁻¹, respectively. The levels are predicted to reach 750 ppm CO₂ and 200 Tg N yr⁻¹ by the end of this century¹⁻⁴. The increases in CO₂ are projected to contribute to global warming and changes in precipitation patterns. According to IPCC reports, global mean temperature has increased by 0.76 °C since 1850 and is predicted to increase between 1.5 °C and 3.2 °C in the coming decades². In high-latitude grasslands, precipitation is also expected to increase⁵. These four global change factors (GCFs) or their combinations can strongly influence terrestrial plant community composition and function^{6, 7}. The GCFs can also directly and indirectly affect soil biological communities that regulate soil nutrient availability, resulting in positive or negative feedback^{8, 9}. However considerable uncertainty remains about how the complex interactions among elevated CO₂, increased precipitation, warming, and N addition affect soil fungi, especially the ubiquitous plant symbionts.

Arbuscular mycorrhizal fungi (AMF) are root symbionts that play important roles in plant species distribution, community diversity, and productivity and therefore in the functioning of ecosystems worldwide¹⁰. They form mutualistic associations with the roots of almost all plant species in grasslands. The AMF supply nutrients (e.g., N and phosphorus) and improve plant resistance to drought stress in exchange for plant-assimilated carbon compounds¹¹. Because of their essential roles, it is particularly important to predict how AMF communities will respond to future changes in the global climate. Increasing CO₂ concentrations can theoretically stimulate plant growth and provide more photosynthesis products to AMF, consequentially modifying the AMF community structure. However, in N-limited grasslands, such stimulation is rarely achieved because of the low availability of soil N¹². Although N deposition increases the N influx to grasslands, precipitation changes and warming can increase or decrease soil N availability. In addition, N addition can alter plant community composition and diversity¹³. The resulting shifts in plant community composition may reduce the negative effects of N addition on the structure and function of AMF communities. Other studies show that warming increases mycorrhizal colonization¹⁴ and AMF diversity¹⁵, and changes the abundance of Glomeraceae and Gigasporaceae¹⁶. The GCFs always occur simultaneously and therefore their interactive effects may affect ecological communities and processes. Although many studies examine how AMF communities respond to atmospheric CO₂ enrichment^{17, 18}, N deposition¹⁸, warming¹⁵, and increased precipitation¹⁹, very few have simultaneously experimentally explored the interactive consequences of these four GCFs on the AMF communities.

Arbuscular mycorrhizal fungi provide nutrients, water, and trace minerals to host plants in exchange for photosynthesis products. Therefore, many studies highlight the importance of plant community types and changes in plant communities in affecting the response of mycorrhizal fungi to climate changes^{17, 18}. Additionally, studies report that abiotic environmental factors, such as soil temperature, moisture, and physiochemical properties, can explain the differences in AMF communities between sites^{20, 21}. These observations indicate that habitat filtering is a driver of AMF community assembly. Apart from the above deterministic processes (homogeneous and variable selection), stochastic processes (ecological drift, homogenizing dispersal, and dispersal

limitation) may also shape AMF community assembly under future global climate change. Arbuscular mycorrhizal fungi are found in every plant habitat. They generally do not produce fruiting bodies but release spores from belowground hyphae. Thus, the dispersal of AMF is likely relatively limited²², although it may depend on soil disturbance and spore size. However, whether global changes can further limit dispersal of AMF and thereby influence plant growth and production remains unknown. According to current ecological theory, ecological deterministic and stochastic processes play important roles in community assembly and dynamics²³. Elucidating the assembly processes of AMF communities under global change at a local scale can help to predict responses of those communities to shifts in climate. Therefore, understanding the degree to which dispersal processes shape AMF communities is important practically in predicting the effects of global changes (e.g., N deposition) and is important theoretically in predicting the fungal symbionts as well as the ability of AMF communities to adapt to local environmental changes.

Previous observations at the study site revealed that CO₂ enrichment did not alter the primary productivity of the plant community but changed its composition²⁴. In addition, warming, increased precipitation, and N addition significantly increased gross ecosystem productivity²⁴, with an interaction effect of warming and precipitation²⁵. Increased precipitation and N addition but not warming altered the composition of AMF community, via the indirect effects on plant community composition^{26,27}. Therefore, N addition and increased precipitation likely had greater effects on AMF communities than warming and CO₂ enrichment. To further examine the effects of the GCFs on the AMF community, the following questions were addressed in this study: (i) what GCF most affects the AMF community; (ii) do interactions among GCFs affect the AMF community; and (iii) what processes dominate the assembly of the AMF community and its response to GCFs? The following hypotheses were proposed: (i) N addition would mostly decrease AMF biomass and significantly change AMF community structure, (ii) the combination of N and CO₂ would cause the most increases and changes in the AMF community, and (iii) dispersal limitation would play a dominant role in shaping AMF community, and variable selection would drive community response to global changes. To address the questions and test the hypotheses, the composition and the soil AMF community was examined in a four-factor GCF experiment conducted in open-top chambers in a semiarid grassland in China.

Materials and methods

Site description and sampling

The experimental site was in semi-arid, temperate steppe in Duolun County (42°02' N, 116°16' E, 1,324 m a.s.l.), Inner Mongolia, China. The Global Change Impacts Experimental Platform (GCIEP)²⁴, was established in May 2011 in order to manipulate four GCFs each at two levels: ambient atmospheric CO₂ concentration (aCO₂) and elevated CO₂ by 200 ppm (eCO₂); ambient precipitation (aP) and 30% above aP (eP); ambient N deposition (aN) and aN plus 10 g of N m⁻² yr⁻¹ (eN); and ambient temperature (aT) and elevated temperature (eT) by nighttime (18:00 to 06:00, local time) warming. A full factorial design was used for CO₂, P, and T with eight treatment combinations and three replications of each treatment. Twenty-four 4 m × 4 m plots were set up and arranged in six rows and four columns, with a 4-m buffer zone between any two adjacent plots.

In addition, a split-plot design was used to manipulate the two levels of N deposition, in which each of the 24 plots was divided into two subplots, one with N addition and the other without. Therefore, the GCIEP included sixteen treatment combinations in total, including: aCO₂aPaTaN, aCO₂aPaTeN, aCO₂aPeTaN, aCO₂aPeTeN, aCO₂ePaTaN, aCO₂ePaTeN, aCO₂ePeTaN, aCO₂ePeTeN, eCO₂aPaTaN, eCO₂aPaTeN, eCO₂aPeTaN, eCO₂aPeTeN, eCO₂ePaTaN, eCO₂ePaTeN, eCO₂ePeTaN, and eCO₂ePeTeN.

To manipulate CO₂ concentration, 24 octagon, open-top chambers (OTCs; 4 m between any two parallel sides, 2 m in height, and 13.2 m² of ground area enclosed) were constructed using steel frames and optical glass in the 24 4 m × 4 m plots. In addition, to estimate the effect of OTC on air and soil microclimates, three additional OTCs with only the steel frames were built as ambient OTCs. In each eCO₂ plot, pure CO₂ was introduced into the OTC to achieve a diurnal CO₂ enrichment of 200 ppm over ambient air from June to September of each year. The enrichment was controlled by an Li-820 CO₂ test system (LiCor, Lincoln, NE, USA) and an automatic control system (Luzhai Co., Beijing, China). Increased precipitation was applied with an automatic sprinkler system during each natural rain event from June to September of each year to avoid changing rainfall frequency. The application of NH₄NO₃ in mid-June (5 g N m⁻² yr⁻¹) and mid-July (5 g N m⁻² yr⁻¹) of each year mimicked N addition. All 27 OTCs were divided into two subplots, one with N addition and the other without. All the nighttime-warmed plots were heated continuously by 136 W m⁻² of infrared radiation from mid-March to mid-November of each year, using 1.65 m (length) × 0.15 m (width) MSR-2420 infrared radiators (Kalglo Electronics Inc., Bethlehem, PA, USA) suspended 2.75 m above the ground.

In mid-August 2017, three soil cores (diameter 3.8 cm, depth 20 cm) were randomly collected from each subplot and mixed in a sterile bag. The corer was washed with tap and filter-sterilized water and re-sterilized by alcohol lamp between samples. The soil samples were immediately transported in an ice bucket to a nearby field station laboratory. The samples were sieved through a sterilized 2-mm mesh sieve to remove plant roots and rhizomes and any stones or other debris. The 54 samples were stored in a freezer at -80°C.

DNA extraction, PCR amplification and high-throughput sequencing

Total DNA was extracted from three 500-mg subsamples from each soil sample using an E.Z.N.A.® Soil DNA Kit (Omega Bio-tek, Inc. Norcross, GA, USA) according to the manufacturer's instructions. DNA extracts were quantified using a NanoDrop NC2000 Spectrophotometer (Thermo Scientific, Wilmington, DE, USA), and then diluted to 20 ng/μL before polymerase chain reaction (PCR) amplification. All PCRs were performed in an Applied Biosystems 2720 Thermal Cycler (ABI, Foster City, CA, USA). PCR amplification was performed using the AMF-specific primer pair AMV4.5NF (5'-AAGCTCGTAGTTGAATTCG-3') and AMDGR (5'-CCCAACTATCCCTATTAATCAT-3')²⁸. PCR reactions were performed in a reaction volume of 25 μL that contained 5 μL of 5 × reaction buffer, 5 μL of 5 × GC buffer, 2 μL of dNTP (2.5 mM), 1 μL of forward primer (10 μM), 1 μL of reverse primer (10 μM), 2 μL of DNA template, 8.75 μL of ddH₂O and 0.25 μL of Q5® High-Fidelity DNA Polymerase. Before amplification, DNA samples were denatured at 98 °C for 2 min. Next, 30 cycles were run,

consisting of 15 s at 98 °C, 30 s at 55 °C and 30 s at 72 °C, followed by a final elongation of 5 min at 72 °C. After separation of PCR products by gel electrophoresis, amplicons within the appropriate size range were cut from the agarose gel (75510-019, Invitrogen, Paisley, UK), and purified using an AxyPrep DNA Gel Extraction Kit (Axygen Biosciences, Union City, CA, USA). Purified PCR products were quantified using a Quant-iT PicoGreen® dsDNA Assay Kit (Invitrogen, Paisley, UK) and an FLX800T Microplate reader (BioTek, Winooski, USA). Amplicon libraries were prepared using a TruSeq Nano DNA LT Library Prep Kit (Illumina, San Diego, CA, USA). Paired-end (2 × 300 bases) sequencing was performed on an Illumina MiSeq platform using MiSeq Reagent Kit V3 (600 cycles) at Shanghai Personal Biotechnology Co., Ltd. (Shanghai, China).

Real-time fluorescence quantitative PCR

The effects of elevated CO₂, warming, N addition, and increased precipitation on soil fungal and AMF biomass (internal transcribed spacer (ITS) gene copies) were determined using quantitative real-time PCR (qPCR) on a StepOnePlus™ System (ABI, CA, USA) with AceQ® qPCR SYBR® Green Master Mix (Q112-02, Vazyme). The primers ITS1F (5'-TCCGTAGGTGAACCTGCGG-3') and 5.8S (5'-CGCTGCGTTCTTCATCG-3') were used for overall fungal ITS gene amplification, and the primers AMV4.5NF and AMDGR were used for AMF biomarker measurement. Each reaction contained 10 µL of 2 × SYBR real-time PCR premixture and 0.4 µL of each PCR primer (10 µM). Thermocycler conditions included an initial denaturation step at 95 °C for 5 min, and then 40 cycles were performed: 95 °C for 15 s, 60 °C for 30 s, and 72 °C for 30 s. Standard curves were generated with plasmid vectors containing PCR products, and the products were linearized by PCR amplification with the primers followed by purification as previously described. For each qPCR assay, no-template control, standard, and sample reactions were performed in three replications, and a dissociation curve was generated at the end of each run to check product specificity. The fluorescence of SYBR Green was measured at the end of each extension step, and this fluorescence was normalized to that of the ROX reference dye. The efficiency of the overall fungi qPCR assay was 75.52% and that of the AMF qPCR assay was 105.07%, and R^2 values for standard curves were between 0.985 and 0.989 for both genes. The biomarker-based estimate was converted to copy number of each gene in each reaction and normalized to the dry mass of soil dried weight from which DNA was extracted. The biomarker of non-AMF was estimated by the difference between overall fungal and AMF biomass.

Bioinformatics

The raw DNA sequencing data were processed using a combination of QIIME v 1.9.1²⁹, USEARCH³⁰, and UPARSE³¹. First, the ambiguous bases and the homopolymers with more than eight bases were removed to ensure the quality of sequencing data. The remaining sequences were subjected to demultiplexing according to the barcode and index for each sample. Reads were paired and merged with 20-bp minimum overlap and 20% mismatch using USEARCH. Then, UCLUST was used to cluster operational taxonomic units (OTUs) at 97% identity³⁰. The

taxonomic identity of the representative sequence of each OTU was assigned by comparison with the specific repository for the sequences of Glomeromycota in the MaarjAM database ³². Last, the OTU table was rarefied to 7,000 reads per sample for downstream diversity and network analyses.

Data analysis and statistics

First, multivariate analyses of variance (MANOVAs) with a split-plot design were conducted to assess the main and interactive effects of CO₂, N, warming, and precipitation on overall soil fungal ITS gene, AMF biomarker gene, and non-AMF biomarker gene copies. Before analysis, the data were checked for normality (*shapiro.test* function in R) and homogeneity of variances (Levene's test).

Chao1 and Simpson's indices were used to measure richness and evenness, respectively, of AM fungal communities and were calculated using the R-package *vegan* ³³. Richness and Faith's phylogenetic diversity (PD) index were used to describe the compositional diversity of AMF communities and were calculated using the R-packages *vegan* ³³ and *Picante* ³⁴. Shannon and Allen (ChaoPD) indices were used to assess the structural diversity of AMF communities on the basis of relative abundance of OTUs and phylogenetic lineages, respectively, and were calculated using the *diversity* and *ChaoPD* functions of the R-package *vegan* and *entropart*, respectively. The main and interactive effects of CO₂, N, warming, and precipitation on these four indices were assessed by MANOVAs. Additionally, the four indices were used to assess the dissimilarity of AMF communities under the four GCFs and their interactions. Sorensen and phyloSor dissimilarity indices were used to measure taxonomic and phylogenetic compositional dissimilarity, respectively, among AMF communities, and Shannon and Allen indices were used to determine the taxonomic and phylogenetic structural dissimilarity, respectively, among AMF communities. These four indices were calculated using the R-package *betapart* ³⁵.

To compare the AMF community composition among the four main factors and the sixteen treatments, Venn diagrams were generated using the R-package *UpSetR* and *VennDiagram*. To identify taxa that were specific to one type of GCF treatment, the differentially abundant taxa were determined by linear discriminant analysis effect size (LEfSe) via the Galaxy server (<http://huttenhower.sph.harvard.edu/galaxy/>).

To examine differences in AMF communities between ambient and elevated levels of CO₂ concentration, N addition, warming, and precipitation, first, principal coordinate analysis (PCoA) was performed using Bray-Curtis and Jaccard distances with the *ordinate* function in the R-package *vegan*. Next, whether soil AMF communities differed in main and interactive effects of the four GCFs was explicitly tested with four-way PERMANOVA (999 permutations) using the *adonis* function in the R-package *vegan*. To assess whether the four GCFs and their interactions influenced the phylogenetic structure of soil AMF communities, a four-way PERMANOVA (999 permutations) was conducted based on weighted and unweighted UniFrac distances using the *distance* function of the *phyloseq* package and the *adonis* function of the *vegan* package in R.

To evaluate the processes that contributed to the assembly of AMF communities under the four GCFs, the β -nearest taxon index (β NTI) was used to quantify the phylogenetic turnover between communities. This ecological community modeling framework was developed to assess the relative contributions of stochastic and deterministic processes to the assembly of microbial communities ^{36, 37}. The β NTI was estimated by comparing the observed β -mean nearest taxon

distance (β MNTD) with the mean of a null distribution of β MNTD (999 randomizations), and by normalizing its standard deviation using “*comdistnt*” in the R-package *picante* (Stegen et al., 2012, 2015). The relative extent to which AMF community assembly was governed by deterministic processes (homogeneous or variable selections) was determined by evaluating the percentage of all pairwise β NTI values that fell below -2 or above $+2$, respectively³⁶. By contrast, when $-2 < \beta$ NTI $< +2$, stochastic processes played an important role. Furthermore, to identify the relative contributions of stochastic processes (homogenizing dispersal, dispersal limitation, and ecological drift), the outcome of the β NTI analyses was combined with a second null model, Raup-Crick (RC_{bray}) which is based on a Bray-Curtis metric adapted to account for species’ relative abundances³⁶. The relative contribution of dispersal limitation was defined by the percentage of pairwise values that met the conditions $-2 < \beta$ NTI < 2 and $RC_{\text{bray}} > 0.95$. The relative contribution of homogenizing dispersal was estimated by the percentage of pairwise values that met the conditions $-2 < \beta$ NTI < 2 , and $RC_{\text{bray}} < -0.95$. Last, the undominated process (i.e., ecological drift) governing AMF community composition assembly was estimated by the percentage of pairwise values that met the conditions $-2 < \beta$ NTI $< +2$ and $-0.95 < RC_{\text{bray}} < +0.95$.

The microbial-association network between pairs of AMF OTUs for each GCF across 24 subplots was constructed using abundant OTUs that were in at least nine samples. The SParse Inverse Covariance Estimation for Ecological Association Inference (SPIEC-EASI) framework³⁸, a statistical method that is robust to all issues of compositional data encountered in microbiota analysis, was used to infer the microbial ecological networks in OTU data sets. Network topology features were characterized by average stability of sparsity, index of the selected *lambda* from the provided *lambda* path (INDLLP), penalty parameter from the provided *lambda* path (PPPL), average nearest neighbor degree (ANND), average path length, betweenness centrality, closeness centrality, degree assortativity, clustering coefficient, degree centralization, density, transitivity, number of vertices, number of edges, modularity, diameter, number of clusters, and mean distance with the R-package *igraph*. Topological roles of interconnecting AMF OTUs in the same and different modules were calculated according to³⁹. To identify the topological properties of each node within an AMF co-occurrence network, each network was separated into modules by comparing the differences between the topological indices of empirical and random networks with the parameters of within-module connectivity (Z_i) and among-module connectivity (P_i) using the R- packages *bipartite* and *microbiomeSeq*.

Availability of data and materials

Data sets of AMF biomarker sequences are archived at the National Center for Biotechnology Information Sequence Read Archive (<https://www.ncbi.nlm.nih.gov/>) under BioProject ID PRJNA701203.

Results

The main effects of CO₂, N, T, and P did not significantly affect the biomass of total soil, AMF, or saprophytic fungi in this study (Table 1). Only a marginally significant interaction effect of the four GCFs on total fungal biomass was observed ($p < 0.1$), and there was no significant

interaction effect on AMF biomass. Nitrogen deposition only decreased AMF biomass when the system was under combined eCO₂ and eT (two tail T-test, $p < 0.01$, Fig. S1). Nitrogen addition also reduced total fungal biomass under aCO₂ and aT, independent of precipitation, which showed a contrasting effect under eCO₂ (Fig. S1). Under eN, a marginally significant increase in saprophytic and total fungal biomass was observed under eCO₂ and eT as well as under their interaction, whereas these two factors had no additive effect on the biomass of either fungal group (Fig. 1).

Paraglomus and *Glomus* were the dominant genera in this study (Fig. 2 and Fig. S2). The relative abundance of *Paraglomus* under N addition was commonly higher than that under aN across treatments, whereas the relative abundance of *Glomus* decreased, especially under the combination of warming and eCO₂ (Fig. 2 and Fig. S2). Ninety-eight OTUs were shared across the sixteen treatments (Fig. S3).

There were some main effects of P, T and N on Faith's diversity (PD) and ChaoPD, as well as some effects of the three-way interaction among CO₂, T and N on Chao1, richness, and phylogenetic diversity. The ChaoPD of the AMF community increased under eN ($p < 0.05$) (Fig. 3a) but decreased under eP ($p < 0.05$) and eT ($p < 0.1$) (Fig. 3b, f). Warming decreased Chao1 diversity and richness ($p < 0.05$; Fig. 3c, d) and also Faith's PD ($p < 0.01$; Fig. 3e) in addition to significantly increasing phylogenetic clustering alone and combined with CO₂, N, and P (Figure S2). Under eCO₂, N addition increased richness and Chao1 diversity but only under aT (Fig. 4a, b and 4g, h); while under eN, eCO₂ increased Chao1 and Faith's PD diversity but only under aT (Fig. 4c, d and 4e, f).

Principal coordinate analyses revealed significant separation in AMF community composition (based on Bray-Curtis, Jaccard, and UniFrac, and weighted UniFrac distances) between the aN and eN treatments (Fig. 5, Table 2). Arbuscular mycorrhizal fungal community composition was not significantly different between aCO₂ and eCO₂, or between aP and eP, but was between aT and eT for the case based on unweighted UniFrac distance (Table 2). The interaction between P and T based on unweighted UniFrac distance significantly affected AMF community composition. In addition, some marginally significant interaction effects between warming and N addition affected AMF community composition (Table 2, Fig. S4).

The LEfSe revealed that the OTUs classified within the genera *Diversispora*, *Scutellospora*, and *Claroideoglomus* were more abundant under aT (Fig. 6). Two OTUs within the genera *Glomus* and *Septoglomus* were identified as indicators of the N addition across all samples, whereas only one OTU within *Paraglomus* was identified as an indicator of ambient soil N.

Edges were predominantly composed of strong positive associations in the eCO₂, eN and eP networks, in contrast to those in the eT network, and the dominant, identifiable OTUs belonged to the genus *Glomus* (Fig. S5). Elevated CO₂, eN, and eP increased the closeness centrality of networks, whereas eT decreased the closeness centrality, number of vertices, and number of edges (Table 3). Many AMF OTUs in this study were connectors, with only a few were peripherals (specialists) found in the eCO₂ and aCO₂ co-occurrence networks (Fig. 7, Fig. S5 and S6). As examples, several peripheral OTUs of the genus *Glomus* were observed that were not found in the eCO₂ network (Fig. 7a), whereas an OTU of the genus *Archaeospora* was peripheral (Fig. 7b).

The median value of the β NTI had an absolute value of $<+2$ under the main factor treatments, and many β NTI values were greater than $+2$ (Fig. 8a). Most β NTI values fell within the range of -2 to $+2$ across the sixteen combination treatments (Fig. 8b). Homogeneous selection and

homogenizing dispersal had almost no influence on the AMF community assembly in this study site. Elevated CO₂ and warming treatment decreased the phylogenetic turnover of AMF communities, whereas warming increased the turnover (Fig. S7). Furthermore, the β -NTI values were always lower in eN combinations with other factors than in aN combinations. The percentage contribution of variable selection decreased with eCO₂, eN and warming, but increased with eP (Fig. 8c). Decreases in the contribution of dispersal limitation occurred with eCO₂, warming, and eP, but increases occurred with eN. Elevated N influenced the community assembly of AMF when averaged across the four treatment combinations with eCO₂, eT, and with aP, respectively (Fig. 8c and d).

Discussions

CO₂ enrichment positively affected the saprophytic fungal community

In a previous study at this four-factor OTC experimental facility, eCO₂ did not affect net ecosystem productivity²⁴. The lack of response in net ecosystem productivity to CO₂ enrichment was attributed to increases in soil respiration offsetting ecosystem C uptake. Therefore, eCO₂ could have increased soil total fungal and AMF biomass, indicating critical roles for fungal communities in the carbon-cycling response to CO₂ enrichment. Many previous studies demonstrate that short-term eCO₂ increases gross ecosystem productivity^{10,40}, which suggests that more substrate is available for AMF and saprophytic fungi because of increased carbon input to soil. In this study, CO₂ increased total fungal biomass depending on N level and temperature. Furthermore, the increases were attributed to changes in saprophytic fungi and not in AMF. Changes in plant community composition are one mechanism that might explain the absence of responses by AMF biomass to CO₂ enrichment and its interaction with other factors in this study. At the study site, the plant canopy did not respond to eCO₂ under any treatment combinations from 2014 to 2017, whereas forb cover increased by 8.6% with eCO₂²⁴. Notably, an increase in the forb:grass ratio is associated with increases in saprophytic fungi rather than AMF⁴¹.

Nitrogen addition predominantly influenced the β -diversity of AMF community

Nitrogen addition can significantly affect AMF community composition and, depending on the ecosystem, can have a negative or no effect on AMF biomass^{26,42}. In a two-factor experiment conducted in the same site as this study, Kim et al. (2015) found N addition significantly decreased AMF extraradical hyphal biomass, despite warming²⁶. In this study, N addition significantly decreased AMF biomass only with eCO₂ and warming, although N addition tended to decrease AMF biomass. Furthermore, the effect of N addition on AMF community composition was greater than that of eCO₂, eP and eT. These results are consistent with the hypothesis in this study and suggest that N deposition is an important GCF in this semiarid grassland, although its effects are also dependent on other GCFs. The relative abundance of genus *Paraglomus* under N addition was frequently higher than that under aN across treatments, whereas the relative abundance of *Glomus* was lower, especially under combined eT and eCO₂ (Figure 2 and Figure S2). Two OTUs within *Glomus* and *Septoglomus* were identified as indicators of N addition across all samples, whereas only one OTU within *Paraglomus* was identified as an indicator of ambient N. On the basis of these results, host specificity should be determined to confirm the sensitivity of these AMF species to active soil N in future studies.

At the study site, the dominant genera *Paraglomus* and *Glomus* are rhizophilic AMF.

Rhizophylic AMF are likely tolerant of low soil moisture because of the high allocation to intraradical hyphae and limited investment in extraradical hyphae. Both dominant genera of AMF responded differently to N addition. N addition had a negative effect on *Glomus* but a positive effect on *Paraglomus*. These observations are consistent with previous findings that the relative abundance of *Glomus* is negatively correlated with soil N content and is correlated with alkaline-neutral soils. By contrast, the occurrence of *Paraglomus* is correlated with more acidic soils^{42, 43}. Other studies also show that N addition mostly reduces the richness and abundance of the dominant genus *Glomus* and favors other AMF⁴⁴. The difference in response to N addition by *Glomus* and *Paraglomus* might be due to differences in the morphological structure of the mycorrhizal association with plant roots. *Paraglomus* does not have vesicles, and the intraradical hyphae are frequently coiled within and between cortical cells. By contrast, *Glomus* frequently contains vesicles and rarely produces coils in its mycorrhizal association. A decrease in vesicles with high N addition was also observed in a field study⁴⁵.

Warming predominantly influenced the phylogenetic diversity of AMF

The alpha diversity of AMF communities was likely to be lower in the warming treatment. This result is consistent with those of studies in other grasslands^{46, 47}. By contrary, in a study conducted at the same site as this study, the alpha diversity of the AMF community increased in response to four years of warming²⁶. Some studies also indicate that ecosystem warming may have positive effects on AMF communities by stimulating more carbon allocation to roots in the short term, e.g., after one year of warming¹⁴. By contrast, warming always causes nonsignificant or negative effects on AMF biomass or OTU richness in the long term compared with the ambient temperature treatment. Moreover, warming-caused drought can reduce the allocation of photosynthates to the plant rhizosphere in long-term experiments. In addition, in previous studies, water availability influences aboveground productivity and further affects AMF abundance and diversity⁴⁸. Therefore, these results suggest that the effects of warming on AMF communities are dependent on the temporal scale. Additionally, because the eT network was less connected with low closeness centrality and had fewer vertices and edges; it would be slowly affected by environmental changes. Thus, the implication is that AMF communities can resist even stronger global changes.

Simultaneously, AMF OTUs were also more phylogenetically clustered, and the communities showed lower phylogenetic turnover under warming. By contrast, under aT, distantly related species co-occurred less frequently, and there was high phylogenetic turnover among plots. It is unlikely that warming directly influenced the phylogenetic diversity of AMF communities because they commonly have relatively wide temperature tolerance. Several processes should always be considered when explaining the indirect effects on AMF via their host plants. First, there might be some type of ecological sorting between aT and eT OTCs related to soil properties. For example, reductions in soil water availability due to plant transpiration could drive changes in the abundance and community composition of AMF⁴⁹. A second possibility was that plant community composition changed significantly between aT and eT treatments²⁴. At the same study site, [Yang et al. \(2011\)](#) observed that experimental warming markedly decreased grass community coverage and species richness⁵⁰. It has been demonstrated that the composition of the AMF community in the site was associated with the community composition of the plant community⁵¹. A third possibility was that warming prolonged the period of active plant growth and increased plant productivity, which would increase substrate deposition for AMF. The warming treatment in the

OTCs experiment had certainly improved gross ecosystem productivity ²⁴. Thus, the shifts in phylogenetic patterns in the present study were likely to be caused by altered host plant carbon allocation.

Increasing precipitation had a minor effect on the phylogenetic α -diversity of AMF

Most studies show that increases in precipitation can directly affect AMF biomass by ameliorating water limitation and can indirectly influence AMF species richness and community structure by driving changes in the plant community (e.g., ⁵²). In this study, although the taxonomic structure of AMF communities was not significantly altered by eP, the phylogenetic alpha diversity (Allen index) was significantly lower and the phylogenetic turnover was remarkably higher across the eP treatments. Increased precipitation may affect AMF community assembly by regulating the percentage of AMF root colonization and the assemblage of different lineages. Increases in water availability can directly influence the growth and distribution of AMF extraradical mycelia in semiarid grasslands. Alternatively, increased precipitation may also indirectly affect AMF phylogenetic lineages via changes in plant community composition ⁵³, coverage ⁵², diversity ⁵⁴, and productivity ⁵⁵. Different plant–AMF symbiotic combinations respond differently to changes in the soil matrix water potential ⁵⁶, and therefore, changes in plant communities associated with increased precipitation can potentially feedback to influence the dynamics of AMF communities and their symbiotic associations. When soil water is abundant, AMF lineages that are less efficient in supplying water but more demanding of carbon may be abandoned, with host plants absorbing water via the osmotic potential of root cells. Arbuscular mycorrhizal fungal lineages also vary in their adaptability to drought and water availability, and the lineages with better adaptability to a moisture niche are expected to replace those that are poorly adapted to drought conditions ⁵⁷. In fact, the ability of some AMF species to colonize plants increases under high soil moisture ⁵². Overall, the results suggest that increased precipitation in semiarid grassland will drive changes in AMF phylogenetic alpha diversity in a future warmer world with eCO₂ and eN.

Interactive effects of warming, N addition, elevated CO₂, and increased precipitation on AMF communities

Because the GCFs elevated CO₂, N deposition, warming, and increased precipitation do not occur in isolation, how the interactions of these factors affect soil fungal communities needs to be considered. In this study, N was the predominant GCF to affect the α and β -diversity of AMF communities. Marginally significant interactions between N and CO₂ and between N and CO₂ and warming affected saprophytic fungal biomass, but significant interactions did not affect AMF biomass. Similarly, in a previous study at the same site, significant interaction between CO₂ and N addition and warming did not affect the densities of AMF spores and extraradical hyphae ¹⁵. One mini-review concludes that the interactions of GCFs can lead to non-additive effects ⁵⁸, whereas other meta-analysis studies find that synergistic or antagonistic effects are relatively rare ^{59, 60}. In studies of the interactions between N fertilization and eCO₂, eCO₂ did not change the N-fertilization effect on AMF biomass, in some ecosystems ⁶¹. For example, [Gamper et al. \(2004\)](#) reported that N addition and eCO₂ interactions are not significant for the parameters of AMF communities¹².

Although four-way interactions were not detected in this study, some three-way interactions among CO₂, temperature, and N affected the Chao1, richness, and phylogenetic diversity of AMF

communities. Similar interactive effects on grassland net primary production have also been detected⁶². Because few experiments incorporate the interactive effects of the four GCFs on AMF, it was difficult to link the experimental data in the study with responses worldwide. The ChaoPD of the AMF community increased with N addition but decreased with eP and eT. Warming increased Chao1, richness, and Faith's PD, in addition to significantly increasing phylogenetic clustering alone and combined with CO₂, N, and precipitation. Under eCO₂, N addition increased the richness and Chao1 but only at aT, with no significant interaction at eT. However, when those two treatments were combined, the effects of N almost disappeared. Because AMF are functionally diverse⁶³, a diverse phylogenetic cluster provides varying benefits to a host plant. Changes in AMF community composition in response to interactions of GCFs may significantly influence the composition of plant communities and their productivity in semiarid grasslands. For example, some studies suggest that changes in the composition of AMF communities can cause positive feedback on plant growth^{64, 65}. In the grassland ecosystem of this study, the most abundant AMF groups associated with the dominant plant species varied in their responses to the GCFs⁶⁶. Therefore, models used to predict conditions in future grassland ecosystems must consider the interactions of GCFs and their effects on both plants and their AMF associations.

Effects of GCFs on assembly of AMF communities

Because the functional traits of AMF are phylogenetically conserved⁶⁷, the ecological processes (i.e., deterministic and stochastic processes) governing AMF community assembly can be deduced using the null model^{36, 37}. In this study, variable selection and dispersal limitation played major roles in shaping AMF communities. In some studies, homogenizing dispersal is the dominant process in the assembly of microbial communities, whereas in this study, its contribution to AMF community assembly was minimal. The high dispersal rates associated with homogenizing dispersal would lead to similar composition in microbial communities within one site or habitat⁶⁸. In this study, weak homogenizing dispersal could explain why only 98 OTUs were shared across the sixteen treatments. Homogenizing dispersal always strongly homogenizes soil bacterial communities and results in high similarity in composition. For example, [Luan et al. \(2020\)](#) found homogenizing dispersal is primarily responsible for the turnover and assembly of soil bacterial communities⁶⁹. However, its role in the small-scale spatial assembly of AMF communities remains uncertain. In this study, the faint signal for homogenizing dispersal was accompanied by a strong signal for dispersal limitation, indicating very restricted movement of AMF. These results support the expectation of the study and are consistent with those of other studies⁷⁰, suggesting that dispersal limitation plays important roles in the assembly of AMF communities. Therefore, a likely explanation for the observed assembly pattern is that the relatively large AMF spores in the grassland subsoil are frequently unsuitable for passive wind dispersal. In addition, in the perennial grassland examined in this study, several AMF taxa rarely sporulate, which would limit dispersal. Such high dispersal limitation may increase the proportion of maladapted taxa in AMF communities and thereby increase the vulnerability of plant communities to global changes.

The deterministic processes were weaker in the eCO₂ plots than in the aCO₂ plots when eCO₂ was combined with the other three factors, and variable selection was the primary deterministic process. Variable selection usually causes biotic community dissimilarity because of differences in abiotic and biotic environments⁷¹. In this study, the AMF community assembled with lower turnover in composition under eCO₂ than under aCO₂ across aN, eN, aT, eT, aP, and eP treatments.

This result suggested that eCO₂ may weakened the shift in environmental factors, both biotic and abiotic, caused by eN, eT, and eP. A similar weakening was also found with eN and eT but not with eP. The increase in the variable selection under eP suggested that increased precipitation could strengthen the effects of eN, eT, and eCO₂ on AMF community assembly. These results partially support the hypothesis that variable selection would play a dominant role in affecting the response of AMF communities to global changes. A recent study showed that warming by ~3 °C can increase homogeneous selection because of a positive response by a group of ubiquitous gram-positive bacteria in a temperate grassland⁷². In this study, homogeneous selection for AMF assemblages also increased under warming. The shift in phylogenetic structure of the AMF communities in aT and eT treatments was tightly linked to a large decrease in relative abundance of *Diversispora*, *Scutellospora*, and *Claroideoglossum*. Whereas the percentage of dispersal limitation decreased under eCO₂, eT, and eP, it increased under eN. Given only few of the abundant AMF OTUs in present study act as specialists. The shift could be dominantly due to the ecological drift and dispersal limitation, and partly was attributed to variable selection. The percentage of ecological drift increased under warming and eCO₂, suggesting that in the future, AMF communities in the semiarid grassland might continue to be under a weak homogeneous selection assembly process, regardless of whether alone or in combination with elevated N and precipitation. In this study, stochastic processes increased with N addition, which contrasts with observations of microbial guilds from century-long fertilization plots at Rothamsted Experimental Station⁴³. These results and those of Liu et al. (2017) imply that the duration and strength of N addition play important roles in determining soil microbial communities⁷³. The results of this study also suggest that the interactions among the four GCFs can alter the processes of AMF community assembly. Collectively, the results indicated that both stochastic and deterministic processes determined the responses of AMF assemblages to global changes; however, both processes were context dependent, implying that be a more complex mechanism likely structures the AMF communities than simply host plant community composition.

Conclusions

The effects of four GCFs on the composition of AMF communities were examined in an OTC field experiment in a semiarid grassland in China. Elevated CO₂, warming, N addition, and increased precipitation influenced different aspects of AMF communities. However, the structure and assembly of AMF communities indicated they could resist global changes, particularly with respect to the role played by ecological drift. Future efforts should examine the selection factors that filter the sensitive taxa in plant–fungi symbioses. In particular, identifying the taxa sensitive to N addition may provide insights and increase understanding of the mechanisms that lead to variation in AMF community structure.

Declarations

Ethics approval and consent to participate

Not applicable.

Consent for publication

Not applicable.

Availability of data and material

Data sets of AMF biomarker sequences are archived at the National Center for Biotechnology Information Sequence Read Archive (<https://www.ncbi.nlm.nih.gov/>) under BioProject ID PRJNA701203.

Competing interests

The authors declare that they have no competing interests.

Funding

This research was financially supported by grants from the National Natural Science Foundation of China (41930643, 41673077 and 41877340) and Key Scientific Research Projects of Henan Province (21B180011).

Authors' contributions

Shijie Han and Shiqiang Wan conceived the presented idea and received important feedback from all co-authors. Field management was carried out by Shiqiang Wan. Sampling collections, DNA preparation and real-time PCR were carried out by Junqiang Zheng, Feirong Ren, Mingming Cui, Shilin Wang, and Cong Wang. MiSeq sequencing process and data analysis were carried by Junqiang Zheng and Feirong Ren. The manuscript was written by Junqiang Zheng with help from Jian Wang and Zhongjie Sun. All authors discussed the methods and results and contributed to the final manuscript.

Acknowledgements

We thank JunJie Kim, Guoyong Li and Dong Wang for their fieldwork.

Authors' information

International Joint Research Laboratory for Global Change Ecology, School of Life Sciences, Henan University, Kaifeng, 475004, Henan, China

Junqiang Zheng, Mingming Cui, Cong Wang, Jian Wang, Shilin Wang, Zhongjie Sun, Feirong Ren, Shijie Han

Yellow River Floodplain Ecosystems Research Station, Henan University, Xingyang, China

Junqiang Zheng, Mingming Cui, Cong Wang, Jian Wang, Shilin Wang, Zhongjie Sun, Feirong Ren, Shijie Han

College of Life Sciences, Institute of Life Science and Green Development, Hebei University, Baoding, 071002, Hebei, China

Shiqiang Wan

References

1. Galloway JN, Townsend AR, Erismann JW, et al. Transformation of the nitrogen cycle: recent trends, questions, and potential solutions. *Science*. May 16 2008;320(5878):889-892.
2. IPCC. Climate Change 2014: Synthesis Report. Contribution of Working Groups I, II and III to the Fifth Assessment Report of the Intergovernmental Panel on Climate Change. 2014.
3. Kanakidou M, Myriokefalitakis S, Daskalakis N, et al. Past, Present and Future Atmospheric Nitrogen Deposition. *J Atmos Sci*. May 2016;73(5):2039-2047.
4. Yang S, Gruber N. The anthropogenic perturbation of the marine nitrogen cycle by atmospheric deposition: Nitrogen cycle feedbacks and the ¹⁵N Haber-Bosch effect. *Global Biogeochemical Cycles*. 2016;30(10):1418-1440.
5. IPCC. *The physical science basis. Contribution of Working Group I to the fifth assessment report of the intergovernmental panel on climate change of the intergovernmental panel on climate change.pdf*. Cambridge, UK; New York, NY: Cambridge University Press. 2013.
6. Bradford MA, Wood SA, Maestre FT, Reynolds JF, Warren RJ, 2nd. Contingency in ecosystem but not plant community response to multiple global change factors. *New Phytol*. Oct 2012;196(2):462-471.
7. Franklin J, Serra-Diaz JM, Syphard AD, Regan HM. Global change and terrestrial plant community dynamics. *Proc Natl Acad Sci U S A*. Apr 5 2016;113(14):3725-3734.
8. Delgado-Baquerizo M, Eldridge DJ, Ochoa V, Gozalo B, Singh BK, Maestre FT. Soil microbial communities drive the resistance of ecosystem multifunctionality to global change in drylands across the globe. *Ecol Lett*. Oct 2017;20(10):1295-1305.
9. Zhou Z, Wang C, Luo Y. Meta-analysis of the impacts of global change factors on soil microbial diversity and functionality. *Nat Commun*. Jun 17 2020;11(1):3072.
10. Smith SDH, T.E.; Zhzer, S.F.; Charlet, T.N.; et al. Elevated CO₂ increases productivity and invasive species success in an arid ecosystem.pdf. *NATURE*. 2000;408:4.
11. Veresoglou SD, Rillig MC. Suppression of fungal and nematode plant pathogens through arbuscular mycorrhizal fungi. *Biology Letters*. 2012;8.

12. Gamper H, Peter M, Jansa J, Lüscher A, Hartwig UA, Leuchtman A. Arbuscular mycorrhizal fungi benefit from 7 years of free air CO₂ enrichment in well-fertilized grass and legume monocultures. *Global Change Biology*. 2004;10(2):189-199.
13. Midolo G, Alkemade R, Schipper AM, Benítez - López A, Perring MP, De Vries W. Impacts of nitrogen addition on plant species richness and abundance: A global meta - analysis. *Global Ecol Biogeogr*. 2019;28:16.
14. Rillig MCW, S.F.; Shaw, M.R.; Field, C.B. Artificial climate warming positively affects arbuscular mycorrhizae but decreases soil aggregate water stability in an annual grassland .pdf. *OIKOS*. 2002;97:7.
15. Kim Y, Gao C, Zheng Y, et al. Different responses of arbuscular mycorrhizal fungal community to day-time and night-time warming in a semiarid steppe. *Chinese Science Bulletin*. 2014;59(35):5080-5089.
16. Cao J, Xie L, Zheng Y, Yang Y. Drought intensify the effects of warming on root-colonizing arbuscular mycorrhizal fungal community in subtropical Chinese fir plantation. *Forest Ecology and Management*. 2020;464.
17. Macek I, Clark DR, Sibanc N, et al. Impacts of long-term elevated atmospheric CO₂ concentrations on communities of arbuscular mycorrhizal fungi. *Mol Ecol*. Jul 2019;28(14):3445-3458.
18. Treseder KK. A meta-analysis of mycorrhizal responses to nitrogen, phosphorus, and atmospheric CO₂ in field studies. *New Phytologist*. 2004;164(2):347-355.
19. Herrera J, Poudel R, Nebel KA, Collins SL. Precipitation increases the abundance of some groups of root-associated fungal endophytes in a semiarid grassland. *Ecosphere*. 2011;2(4).
20. Schechter SP, Bruns TD. Edaphic sorting drives arbuscular mycorrhizal fungal community assembly in a serpentine/non-serpentine mosaic landscape. *Ecosphere*. 2012;3(5).
21. Alguacil MDMT, M.P.; Montesinos-Navarro, A.; Roldán, A. Soil characteristics driving arbuscular mycorrhizal fungi communities in semiarid Mediterranean soils. *Appl. Environ. Microbiol*. 2016;82(82):9.
22. Smith SE, Read DJ. *Mycorrhizal symbiosis*. London, UK.: Academic Press; 2008.
23. Zhou JZN, D.L. Stochastic community assembly: Does it matter in microbial ecology.pdf. *Microbiology and Molecular Biology Reviews*. 2017;81(4):17.
24. Song J, Wan S, Piao S, et al. Elevated CO₂ does not stimulate carbon sink in a semi - arid grassland. *Ecol Lett*. 2019;22:11.
25. Wan SX, J.; Liu,W.; Niu, S. Photosynthetic overcompensation under nocturnal warming enhances grassland carbon sequestration. *Ecology*. 2009;90.
26. Kim YC, Gao C, Zheng Y, et al. Arbuscular mycorrhizal fungal community response to warming and nitrogen addition in a semiarid steppe ecosystem. *Mycorrhiza*. May 2015;25(4):267-276.
27. Gao C, Kim YC, Zheng Y, et al. Increased precipitation, rather than warming, exerts a strong influence on arbuscular mycorrhizal fungal community in a semiarid steppe ecosystem. *Botany*. Jun 2016;94(6):459-469.
28. Sato KS, Y.; Saito, M.; Sugawara, K. A new primer for discrimination of arbuscular mycorrhizal fungi with polymerase chain reaction-denature gradient gel electrophoresis. *Grassl. Sci.* . 2005;51:3.
29. Caporaso JGea. QIIME allows analysis of highthroughput community sequencing data.pdf. *Nature Methods*. 2010;7:2.

30. Edgar RC. Search and clustering orders of magnitude faster than BLAST. *Bioinformatics*. Oct 1 2010;26(19):2460-2461.
31. Edgar RC. UPARSE: highly accurate OTU sequences from microbial amplicon reads. *Nat Methods*. 2013;10(10):3.
32. Opik M, Vanatoa A, Vanatoa E, et al. The online database MaarJAM reveals global and ecosystemic distribution patterns in arbuscular mycorrhizal fungi (Glomeromycota). *New Phytol*. Oct 2010;188(1):223-241.
33. Oksanen J, Kindt R, Legendre P, et al. The vegan package. *Community Ecol Package*. 2007;10.
34. Kembel S, Cowan P, Helmus M, et al. Picante: R tools for integrating phylogenies and ecology. *Bioinformatics*. 2010;26.
35. Basega A, Orme DV, S., de Bortoli J, Leprieur F, Logez M. betapart: Partitioning beta diversity into turnover and nestedness components. *R package version 1.5.2*. 2020.
36. Stegen JC, Lin X, Fredrickson JK, Konopka AE. Estimating and mapping ecological processes influencing microbial community assembly. *Front Microbiol*. 2015;6:370.
37. Stegen JC, Lin X, Konopka AE, Fredrickson JK. Stochastic and deterministic assembly processes in subsurface microbial communities. *ISME J*. Sep 2012;6(9):1653-1664.
38. Kurtz ZD, Müller CL, Miraldi ER, Littman DR, Blaser MJ, Bonneau RA. Sparse and Compositionally Robust Inference of Microbial Ecological Networks. *PLoS Comput Biol*. 2015;11(5).
39. Olesen JMB, J.; Dupont, Y.L.; Jordano, P. The modularity of pollination networks.pdf. *PNAS*. 2007;104(50):6.
40. Ryan EM, Ogle K, Peltier D, et al. Gross primary production responses to warming, elevated CO₂, and irrigation: quantifying the drivers of ecosystem physiology in a semiarid grassland. *Glob Chang Biol*. Aug 2017;23(8):3092-3106.
41. Heinen R, Hannula SE, De Long JR, et al. Plant community composition steers grassland vegetation via soil legacy effects. *Ecol Lett*. Jun 2020;23(6):973-982.
42. van Diepen S, Bakal JA, McAlister FA, Ezekowitz JA. Mortality and readmission of patients with heart failure, atrial fibrillation, or coronary artery disease undergoing noncardiac surgery: an analysis of 38 047 patients. *Circulation*. 2011;124(3):8.
43. Liang Y, Ning D, Lu Z, et al. Century long fertilization reduces stochasticity controlling grassland microbial community succession. *Soil Biology and Biochemistry*. 2020;151.
44. Zhao A, Liu L, Xu T, et al. Influences of Canopy Nitrogen and Water Addition on AM Fungal Biodiversity and Community Composition in a Mixed Deciduous Forest of China. *Front Plant Sci*. 2018;9:1842.
45. Egerton-Warburton LMA, E.B. Shifts in arbuscular mycorrhizal communities along an anthropogenic nitrogen deposition gradient.pdf. *Ecological Applications*. 2000;10(2):13.
46. Che R, Wang S, Wang Y, et al. Total and active soil fungal community profiles were significantly altered by six years of warming but not by grazing. *Soil Biology and Biochemistry*. 2019;139.
47. Wilson H, Johnson BR, Bohannan B, Pfeifer-Meister L, Mueller R, Bridgham SD. Experimental warming decreases arbuscular mycorrhizal fungal colonization in prairie plants along a Mediterranean climate gradient. *PeerJ*. 2016;4:e2083.

48. Chen YL, Xu ZW, Xu TL, Veresoglou SD, Yang GW, Chen BD. Nitrogen Deposition and Precipitation Induced Phylogenetic Clustering of Arbuscular Mycorrhizal Fungal Communities. *Soil Biology & Biochemistry*. 2017;115:10.
49. Cregger MA, Schadt CW, McDowell NG, Pockman WT, Classen AT. Response of the soil microbial community to changes in precipitation in a semiarid ecosystem. *Appl Environ Microbiol*. Dec 2012;78(24):8587-8594.
50. Yang H, Wu M, Liu W, Zhang ZHE, Zhang N, Wan S. Community structure and composition in response to climate change in a temperate steppe. *Global Change Biology*. 2011;17(1):452-465.
51. Sun X, Su Y, Zhang Y, et al. Diversity of arbuscular mycorrhizal fungal spore communities and its relations to plants under increased temperature and precipitation in a natural grassland. *Chinese Science Bulletin*. 2013;58(33):4109-4119.
52. Zhang J, Wang F, Che R, et al. Precipitation shapes communities of arbuscular mycorrhizal fungi in Tibetan alpine steppe. *Sci Rep*. Mar 22 2016;6:23488.
53. Sweeney CJ, de Vries FT, van Dongen BE, Bardgett RD. Root traits explain rhizosphere fungal community composition among temperate grassland plant species. *New Phytol*. Oct 1 2020.
54. Xu T, Veresoglou SD, Chen Y, et al. Plant community, geographic distance and abiotic factors play different roles in predicting AMF biogeography at the regional scale in northern China. *Environ Microbiol Rep*. Dec 2016;8(6):1048-1057.
55. Wang H, Ta N, Jin K, et al. Interactive effects of nitrogen fertilizer and altered precipitation on fungal communities in arid grasslands of northern China. *Journal of Soils and Sediments*. 2019;20(3):1344-1356.
56. Jia Y, Shi Z, Chen Z, Walder F, Tian C, Feng G. Soil moisture threshold in controlling above- and belowground community stability in a temperate desert of Central Asia. *Sci Total Environ*. Feb 10 2020;703:134650.
57. Weber SE, Diez JM, Andrews LV, Goulden ML, Aronson EL, Allen MF. Responses of arbuscular mycorrhizal fungi to multiple coinciding global change drivers. *Fungal Ecology*. 2019;40:62-71.
58. Cotton TA. Arbuscular mycorrhizal fungal communities and global change: an uncertain future. *FEMS Microbiol Ecol*. Nov 1 2018;94(11).
59. Yue K, Fornara DA, Yang W, et al. Influence of multiple global change drivers on terrestrial carbon storage: additive effects are common. *Ecol Lett*. May 2017;20(5):663-672.
60. Zhou L, Zhou X, Shao J, et al. Interactive effects of global change factors on soil respiration and its components: a meta-analysis. *Glob Chang Biol*. Sep 2016;22(9):3157-3169.
61. Treseder KK, Allen MF. Mycorrhizal fungi have a potential role in soil carbon storage under elevated CO₂ and nitrogen deposition. *New Phytologist*. 2000;147:12.
62. Zhu K, Chiariello NR, Tobeck T, Fukami T, Field CB. Nonlinear, interacting responses to climate limit grassland production under global change. *Proc Natl Acad Sci U S A*. Sep 20 2016;113(38):10589-10594.
63. Klironomos JN. Variation in plant response to native and exotic arbuscular mycorrhizal fungi.pdf. *Ecology*. 2003;84(9):10.
64. Bever JD. Host-specificity of AM fungal population growth rates can generate feedback on plant growth.pdf. *Plant and Soil*. 2002;244:9.

65. Neuenkamp L, Zobel M, Lind E, Gerz M, Moora M. Arbuscular mycorrhizal fungal community composition determines the competitive response of two grassland forbs. *PLoS One*. 2019;14(7):e0219527.
66. Zheng Z, Ma P, Li J, et al. Arbuscular mycorrhizal fungal communities associated with two dominant species differ in their responses to long - term nitrogen addition in temperate grasslands. *Functional Ecology*. 2018;32(6):1575-1588.
67. Powell JR, Parrent JL, Hart MM, Klironomos JN, Rillig MC, Maherali H. Phylogenetic trait conservatism and the evolution of functional trade-offs in arbuscular mycorrhizal fungi. *Proc Biol Sci*. Dec 7 2009;276(1676):4237-4245.
68. Stegen JC, Lin X, Fredrickson JK, et al. Quantifying community assembly processes and identifying features that impose them. *ISME J*. Nov 2013;7(11):2069-2079.
69. Luan L, Liang C, Chen L, et al. Coupling Bacterial Community Assembly to Microbial Metabolism across Soil Profiles. *mSystems*. Jun 9 2020;5(3).
70. Adams RIM, M.; Taylor, J. W.; Bruns, T. D. Dispersal in microbes: fungi in indoor air are dominated by outdoor air and show dispersal limitation at short distances. *ISME J*. Jul 2013;7(7):1262-1273.
71. Feng Y, Chen R, Stegen JC, et al. Two key features influencing community assembly processes at regional scale: Initial state and degree of change in environmental conditions. *Mol Ecol*. Dec 2018;27(24):5238-5251.
72. Ning D, Yuan M, Wu L, et al. A quantitative framework reveals ecological drivers of grassland microbial community assembly in response to warming. *Nat Commun*. Sep 18 2020;11(1):4717.
73. Liu C, Yao M, Stegen JC, Rui J, Li J, Li X. Long-term nitrogen addition affects the phylogenetic turnover of soil microbial community responding to moisture pulse. *Sci Rep*. Dec 13 2017;7(1):17492.

Figure 1. Three-way interaction effects of ambient (a) and elevated (e) levels of the global change factors nitrogen (N), CO₂, and temperature (T) on **a, b** total fungal biomass and **c, d** saprophytic fungal biomass (log number of ITS gene copies g⁻¹). The *p*-values above the lines are from Tukey's HSD post-hoc tests.

Fig. 2. Relative abundances (%) of major genera of arbuscular mycorrhizal fungi under the influence of ambient and elevated levels of the global change factors nitrogen, CO₂, temperature, and precipitation.

Fig. 3. Significant effects of global change factors on arbuscular mycorrhizal communities. **(a)** Effect of nitrogen (N) addition on ChaoPD (phylogenetic diversity); **(b)** effect of elevated precipitation (P) on ChaoPD; and effect of elevated temperature (T) on **(c)** Chao1, **(d)** richness, **(e)** Faith's PD, and **(f)** ChaoPD. a, ambient level; e, elevated level.

Fig. 4. Three-way interaction effects of global change factors on arbuscular mycorrhizal fungal communities. **a, b** Effect of CO₂, nitrogen (N), and temperature (T) on richness; effect of N, CO₂ and T on **c, d** the Chao1 index and on **e, f** the phylogenetic diversity (PD) index; and **g, h** effect of CO₂, T, and N on the Chao1 index. Ambient (a) and elevated (e) levels.

Fig. 5. Principal coordinate analysis of the effects of nitrogen (N) addition on (a, ambient level; e, elevated level) on variation in arbuscular mycorrhizal fungal community composition. **a** Bray-Curtis distance, **b** Jaccard distance, **c** unweighted UniFrac distance, and **d** weighted UniFrac distances. P, precipitation; T, temperature.

Fig. 6. Discriminant taxa of arbuscular mycorrhizal fungal (AMF) communities as determined by LEfSe analysis in a) warming and unwarmed treatment and b) fertilized and unfertilized treatment. AMF taxa are illustrated according to taxonomic relationships using a cladogram to show the discriminative patterns in taxonomic lineages. c) and d) AMF taxa listed according to linear discriminant analysis (LDA) values. Only the AMF lineages that showed significant responses to eCO₂, eN, eP and eT are shown (a, ambient level; e, elevated level; T, temperature; N, nitrogen; P, precipitation).

Fig. 7. Within-module (*Z_i*) and among-module (*P_i*) connectivity plots showing the distribution of arbuscular mycorrhizal fungi (AMF) based on their topological roles under: a) ambient CO₂ (aCO₂), and b) elevated CO₂ (eCO₂). Each symbol represents an AMF operational taxonomic unit (OTU) (or species). Different symbols indicate different genera. The topological roles of OTUs were determined according to the OTUs interconnecting in the same module (within-module connectivity) and in different modules (among-module connectivity). The OTUs identity numbers label the peripherals. The horizontal and vertical dashed lines represent the threshold values of *Z_i* (2.5) and *P_i* (0.62), respectively, used to categorize OTUs.

Fig. 8. Ecological null model outputs (β NTI) of arbuscular mycorrhizal fungal (AMF) communities under **a)** the eight global change factor (GCF) treatments and under **b)** sixteen GCF treatments. In the box-and-whisker plots, the line in the box represents the median, the top and bottom of the box represent first and third quartiles, respectively, and the whiskers represents the 1.5 interquartile range. **c)** Contributions of community assembly processes governing AMF community turnover under the influence of GCFs. Ambient CO₂ (aCO₂), elevated CO₂ (eCO₂), ambient nitrogen (aN), elevated N (eN), ambient temperature (aT), elevated T (eT), ambient precipitation (aP), elevated P (eP). **d)** Raup-Crick_{Bray-Curtis} results for the AMF communities under sixteen GCF treatments.

Table 1. Summary (P-values) of general linear mixed model on the effects of elevated CO₂ (CO₂), increased precipitation (P), elevated temperature (T) and enriched nitrogen (N) on AMF biomass (AMF), saprophytic fungal biomass (SFungi), total fungal biomass (Fungi), and α -diversity including Shannon, Simpson, Chao1, richness, phylogenetic diversity (PD) and Chao PD index.

Sources of Variation	AMF	SFungi	Fungi	Shannon	Simpson	Chao1	Richness	PD	ChaoPD
CO ₂	0.761	0.243	0.243	0.449	0.275	0.620	0.602	0.939	0.828
P	0.274	0.261	0.239	0.719	0.522	0.727	0.722	0.705	0.049
T	0.912	0.773	0.742	0.377	0.579	0.133	0.118	0.035	0.063
N	0.237	0.934	0.980	0.848	0.997	0.254	0.396	0.797	0.001
CO ₂ ×P	0.960	0.104	0.112	0.188	0.113	0.661	0.768	0.976	0.942
CO ₂ ×T	0.352	0.312	0.289	0.769	0.851	0.798	0.828	0.601	0.326
P×T	0.330	0.539	0.562	0.352	0.532	0.334	0.322	0.093	0.796
CO ₂ ×N	0.936	0.096	0.103	0.657	0.324	0.762	0.644	0.274	0.264
P×N	0.409	0.410	0.424	0.265	0.279	0.243	0.375	0.519	0.713
T×N	0.862	0.277	0.292	0.485	0.580	0.188	0.264	0.397	0.835
CO ₂ ×P×T	0.366	0.373	0.380	0.941	0.861	0.997	0.880	0.876	0.567
CO ₂ ×P×N	0.505	0.405	0.398	0.208	0.319	0.254	0.377	0.167	0.656
CO ₂ ×T×N	0.701	0.077	0.087	0.133	0.361	0.014	0.039	0.048	0.966
P×T×N	0.669	0.733	0.771	0.852	0.939	0.916	0.960	0.776	0.441
CO ₂ ×P×T×N	0.410	0.090	0.092	0.512	0.758	0.255	0.318	0.718	0.762

Note: The bold numerals highlight the significance at $p < 0.1$ or $p < 0.05$ for fungal biomass and α -diversity, respectively. The α -diversity data were performed log-transformations to meet the linear model assumptions.

Table 2. Results of four-way permutational analysis of variance (PERMANOVA) testing effects of CO₂ enrichment, increased precipitation (P), warming (T) and N addition on AMF community.

	Df	unweighted unfrac		weighted unfrac		unweighted OTU		weighted OTU	
		F	P	F	P	F	P	F	P
CO ₂	1	0.925	0.504	0.751	0.560	1.075	0.327	1.075	0.341
P	1	0.834	0.639	1.226	0.244	1.335	0.110	1.335	0.108
T	1	2.728	0.003	1.501	0.158	1.323	0.133	1.323	0.130
N	1	2.717	0.004	3.728	0.01	5.060	0.001	5.060	0.001
CO ₂ ×P	1	0.795	0.732	0.911	0.393	0.829	0.714	0.829	0.708
CO ₂ ×T	1	0.679	0.926	0.703	0.641	1.281	0.141	1.281	0.179
P×T	1	2.001	0.011	0.971	0.416	0.941	0.525	0.941	0.504
CO ₂ ×N	1	0.851	0.638	0.724	0.601	0.883	0.632	0.883	0.629
P×N	1	0.674	0.952	0.710	0.631	0.868	0.679	0.868	0.654
T×N	1	0.951	0.064	1.035	0.074	1.456	0.057	1.456	0.066
CO ₂ ×P×T	1	0.909	0.504	0.700	0.634	0.872	0.637	0.872	0.608
CO ₂ ×P×N	1	1.153	0.222	1.277	0.233	0.905	0.597	0.905	0.570
CO ₂ ×T×N	1	1.158	0.206	1.182	0.247	1.113	0.278	1.113	0.294
P×T×N	1	0.620	0.975	0.538	0.821	1.096	0.297	1.096	0.298
CO ₂ ×P×T×N	1	0.563	0.997	0.343	0.979	0.561	0.988	0.561	0.985

Note: The bold numerals highlight the significance at $p < 0.1$ or $p < 0.05$ for AMF community.

Table 3. Network topology features of SPIEC-EASI network for the four treatments.

	aCO ₂	eCO ₂	aN	eN	aP	eP	aT	eT
Average stability of sparsity	0.043	0.040	0.041	0.044	0.042	0.041	0.039	0.039
INDLLP	4	4	4	4	4	4	4	4
PPPL	0.466	0.458	0.463	0.455	0.462	0.461	0.461	0.463
ANND	4.647	4.864	4.729	5.092	4.778	5.015	4.757	4.492
Average path length	4.304	4.311	4.308	4.166	4.400	4.287	4.457	4.628
Betweenness centrality	0.046	0.047	0.058	0.040	0.049	0.073	0.067	0.063
Closeness centrality	0.062	0.078	0.077	0.117	0.033	0.130	0.132	0.016
Degree assortativity	0.118	0.273	0.112	0.155	0.166	0.144	0.132	0.149
Degree centralization	0.022	0.027	0.025	0.023	0.025	0.029	0.026	0.033
Density	0.018	0.017	0.017	0.018	0.017	0.018	0.015	0.017
Transitivity	0.079	0.086	0.076	0.082	0.091	0.109	0.078	0.092
Number of vertice	225	255	238	248	242	237	274	225
Number of edge	456	537	484	543	494	509	556	424
Modularity	0.565	0.545	0.563	0.545	0.574	0.583	0.572	0.599
Diameter	9	10	10	10	14	10	10	11
Number of clusters	2	2	2	1	4	1	1	5
Mean distance	6.266	6.277	6.272	4.166	12.198	4.287	4.457	21.873

INDLLP: index of the selected lambda from provided lambda path; PPPL: penalty parameter from provided lambda path; ANND: Average nearest neighbor degree.

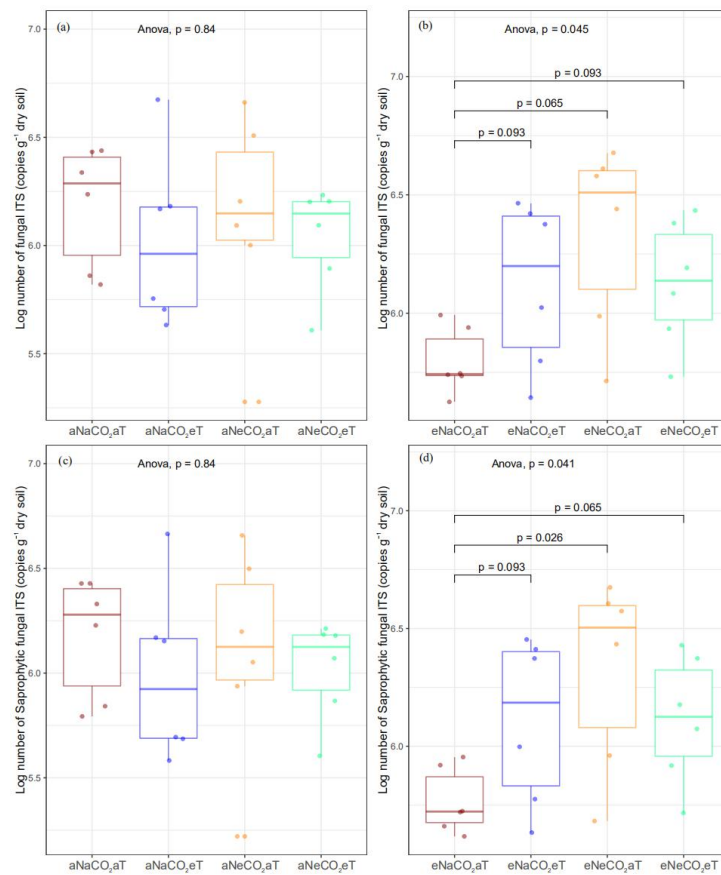


Figure 1. Three-way interaction effects of ambient (a) and elevated (e) levels of the global change factors nitrogen (N), CO₂, and temperature (T) on **a, b** total fungal biomass and **c, d** saprophytic fungal biomass (log number of ITS gene copies g⁻¹). The *p*-values above the lines are from Tukey's HSD post-hoc tests.

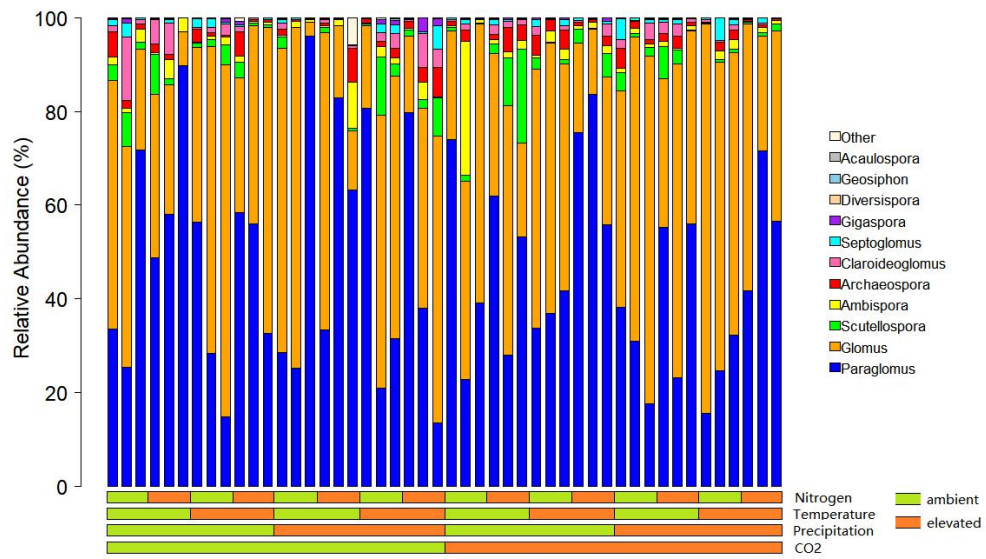


Fig. 2. Relative abundances (%) of major genera of arbuscular mycorrhizal fungi under the influence of ambient and elevated levels of the global change factors nitrogen, CO₂, temperature, and precipitation.

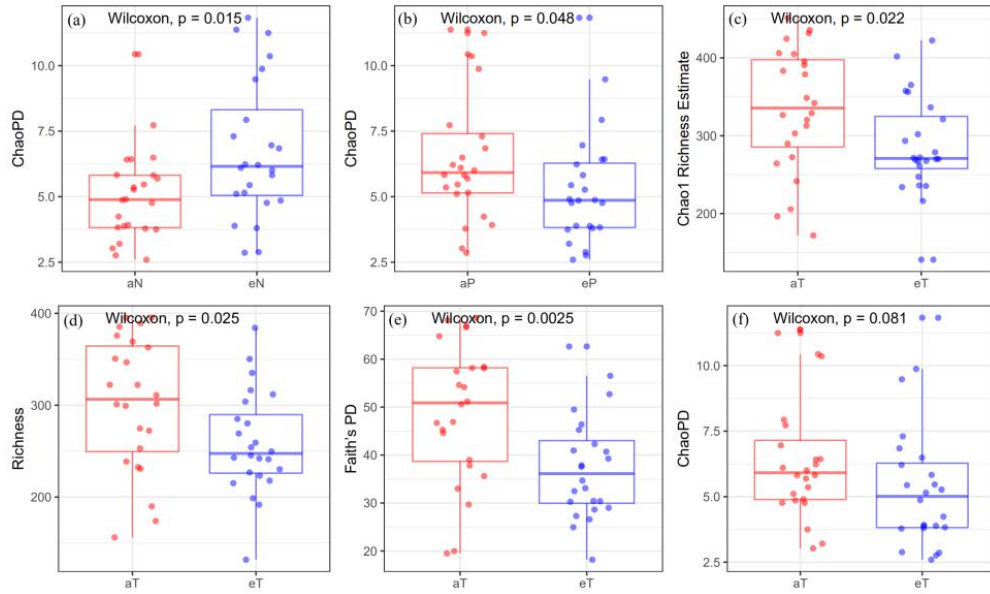


Fig. 3. Significant effects of global change factors on arbuscular mycorrhizal communities. **(a)** Effect of nitrogen (N) addition on ChaoPD (phylogenetic diversity); **(b)** effect of elevated precipitation (P) on ChaoPD; and effect of elevated temperature (T) on **(c)** Chao1, **(d)** richness, **(e)** Faith's PD, and **(f)** ChaoPD. a, ambient level; e, elevated level.

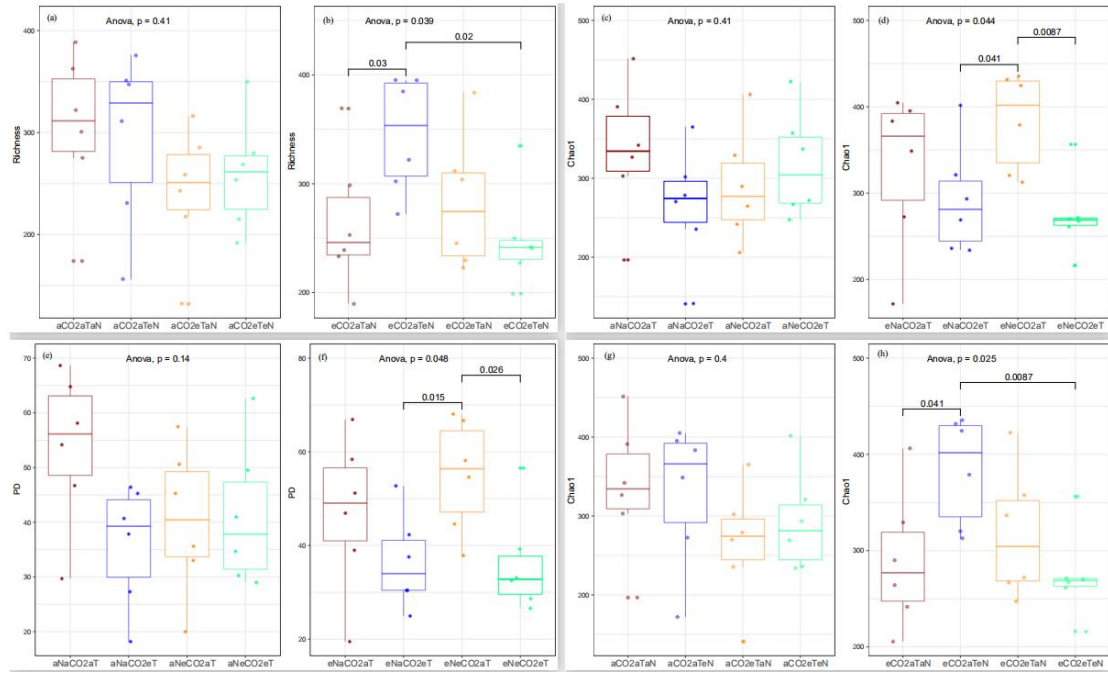


Fig. 4. Three-way interaction effects of global change factors on arbuscular mycorrhizal fungal communities. **a, b** Effect of CO₂, nitrogen (N), and temperature (T) on richness; effect of N, CO₂ and T on **c, d** the Chao1 index and on **e, f** the phylogenetic diversity (PD) index; and **g, h** effect of CO₂, T, and N on the Chao1 index. Ambient (a) and elevated (e) levels.

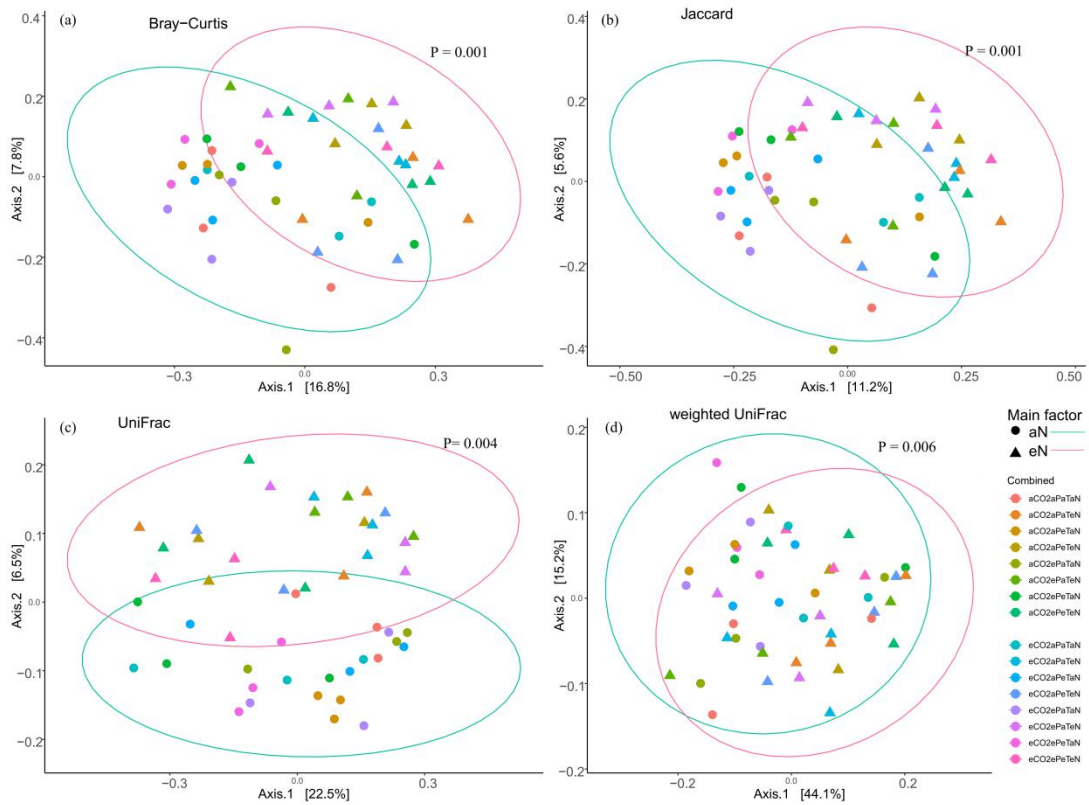


Fig. 5. Principal coordinate analysis of the effects of nitrogen (N) addition on (a, ambient level; e, elevated level) on variation in arbuscular mycorrhizal fungal community composition. **a** Bray-Curtis distance, **b** Jaccard distance, **c** unweighted UniFrac distance, and **d** weighted UniFrac distances. P, precipitation; T, temperature.

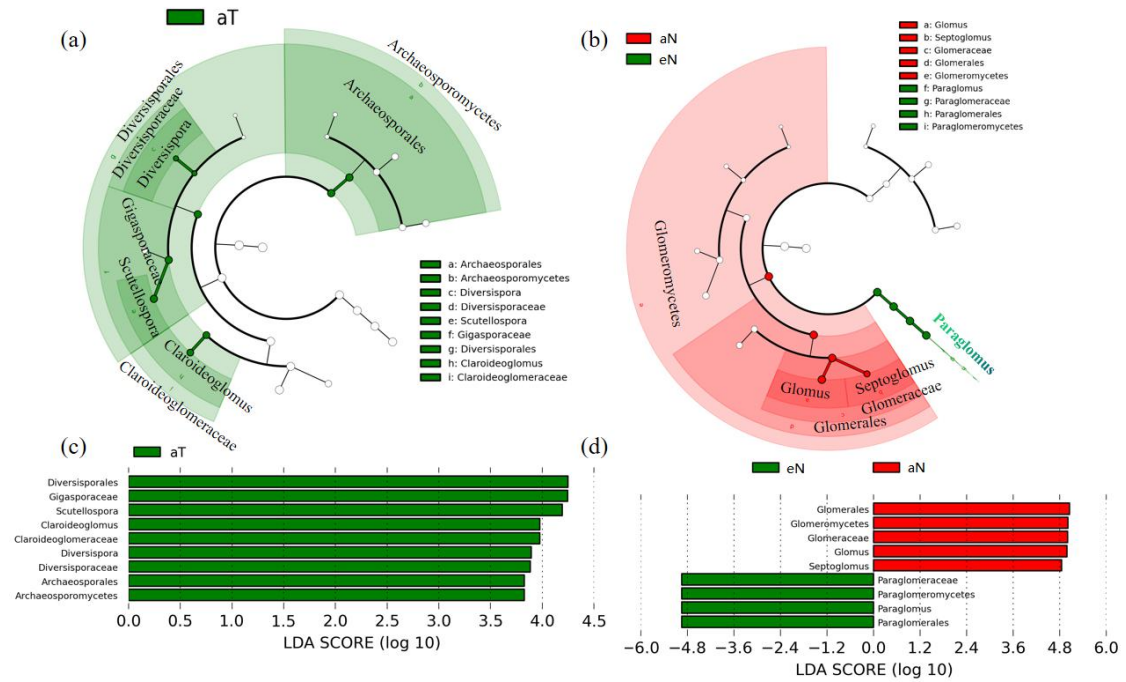


Fig. 6. Discriminant taxa of arbuscular mycorrhizal fungal (AMF) communities as determined by LefSe analysis in a) warming and unwarmed treatment and b) fertilized and unfertilized treatment. AMF taxa are illustrated according to taxonomic relationships using a cladogram to show the discriminative patterns in taxonomic lineages. c) and d) AMF taxa listed according to linear discriminant analysis (LDA) values. Only the AMF lineages that showed significant responses to eCO₂, eN, eP and eT are shown (a, ambient level; e, elevated level; T, temperature; N, nitrogen; P, precipitation).

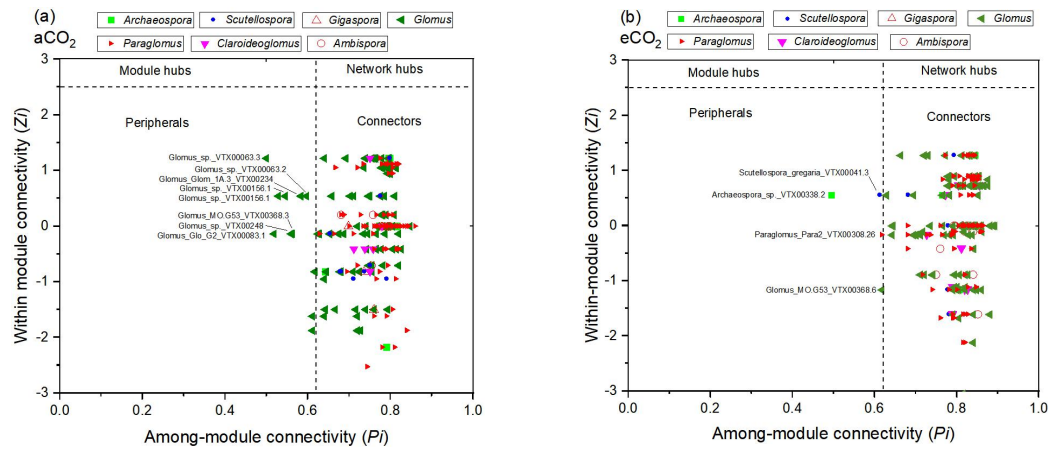


Fig. 7. Within-module (Z_i) and among-module (P_i) connectivity plots showing the distribution of arbuscular mycorrhizal fungi (AMF) based on their topological roles under: a) ambient CO_2 ($a\text{CO}_2$), and b) elevated CO_2 ($e\text{CO}_2$). Each symbol represents an AMF operational taxonomic unit (OTU) (or species). Different symbols indicate different genera. The topological roles of OTUs were determined according to the OTUs interconnecting in the same module (within-module connectivity) and in different modules (among-module connectivity). The OTUs identity numbers label the peripherals. The horizontal and vertical dashed lines represent the threshold values of Z_i (2.5) and P_i (0.62), respectively, used to categorize OTUs.

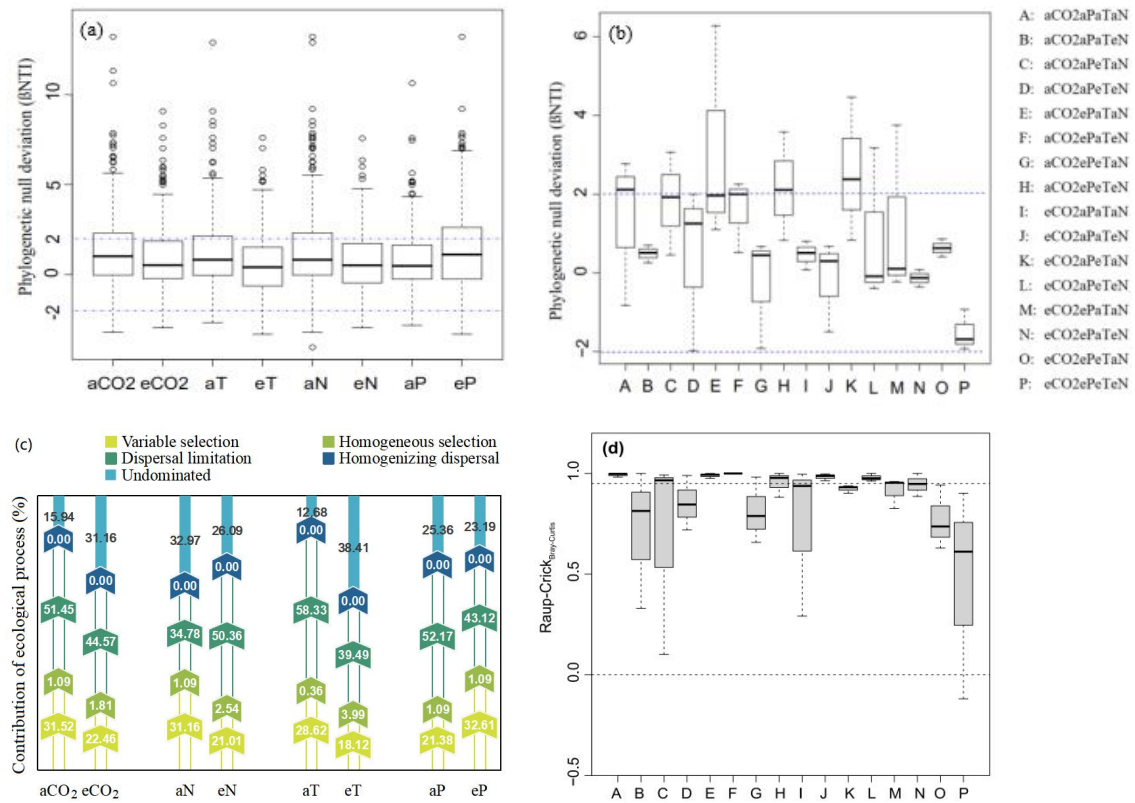


Fig. 8. Ecological null model outputs (β NTI) of arbuscular mycorrhizal fungal (AMF) communities under **a)** the eight global change factor (GCF) treatments and under **b)** sixteen GCF treatments. In the box-and-whisker plots, the line in the box represents the median, the top and bottom of the box represent first and third quartiles, respectively, and the whiskers represents the 1.5 interquartile range. **c)** Contributions of community assembly processes governing AMF community turnover under the influence of GCFs. Ambient CO₂ (aCO₂), elevated CO₂ (eCO₂), ambient nitrogen (aN), elevated N (eN), ambient temperature (aT), elevated T (eT), ambient precipitation (aP), elevated P (eP). **d)** Raup-Crick_{Bray-Curtis} results for the AMF communities under sixteen GCF treatments.

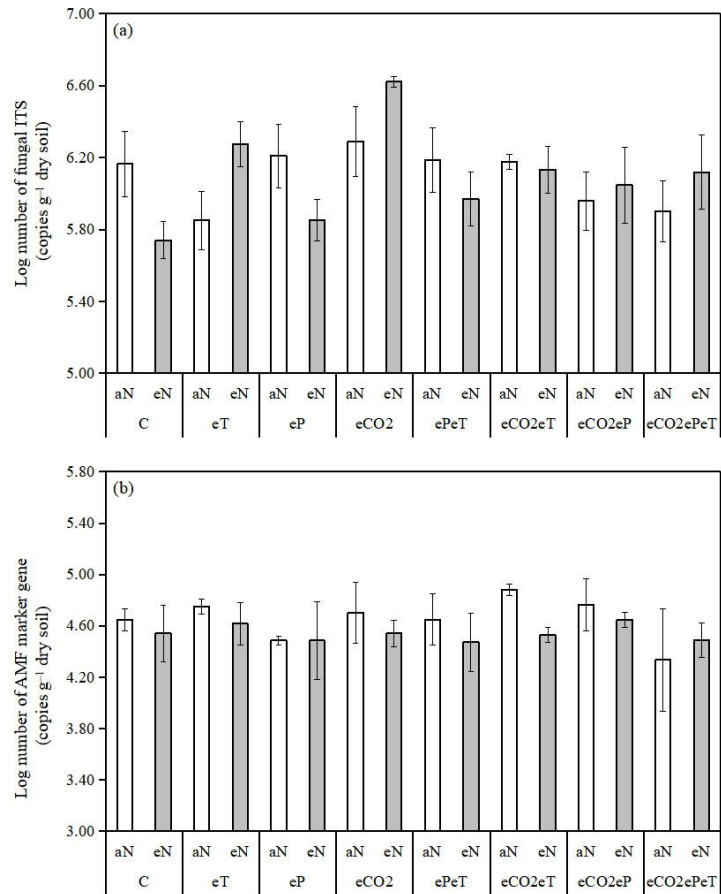


Fig. S1 Quantitative analysis of soil total fungal (a) and AMF (b) biomass based on real-time PCR. Error bars represent standard error (SE) calculated from three independent subplots.

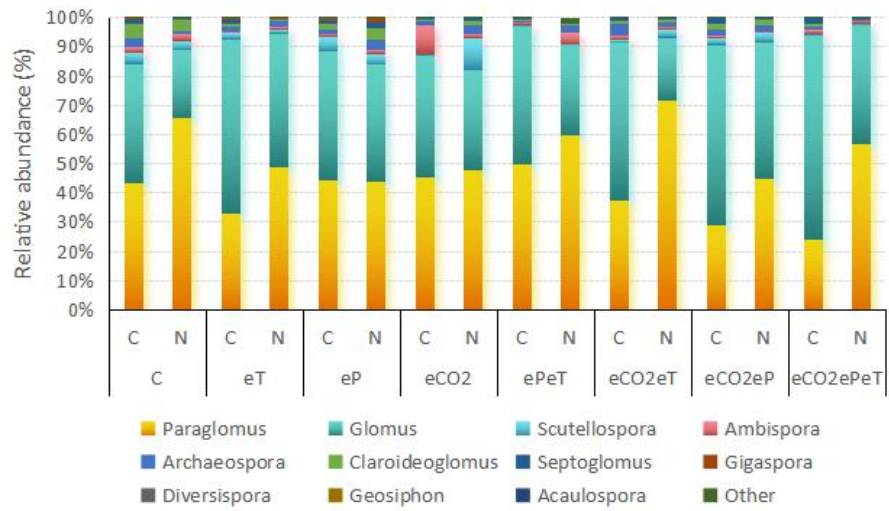


Fig. S2. Relative abundance of AMF communities at genus level.

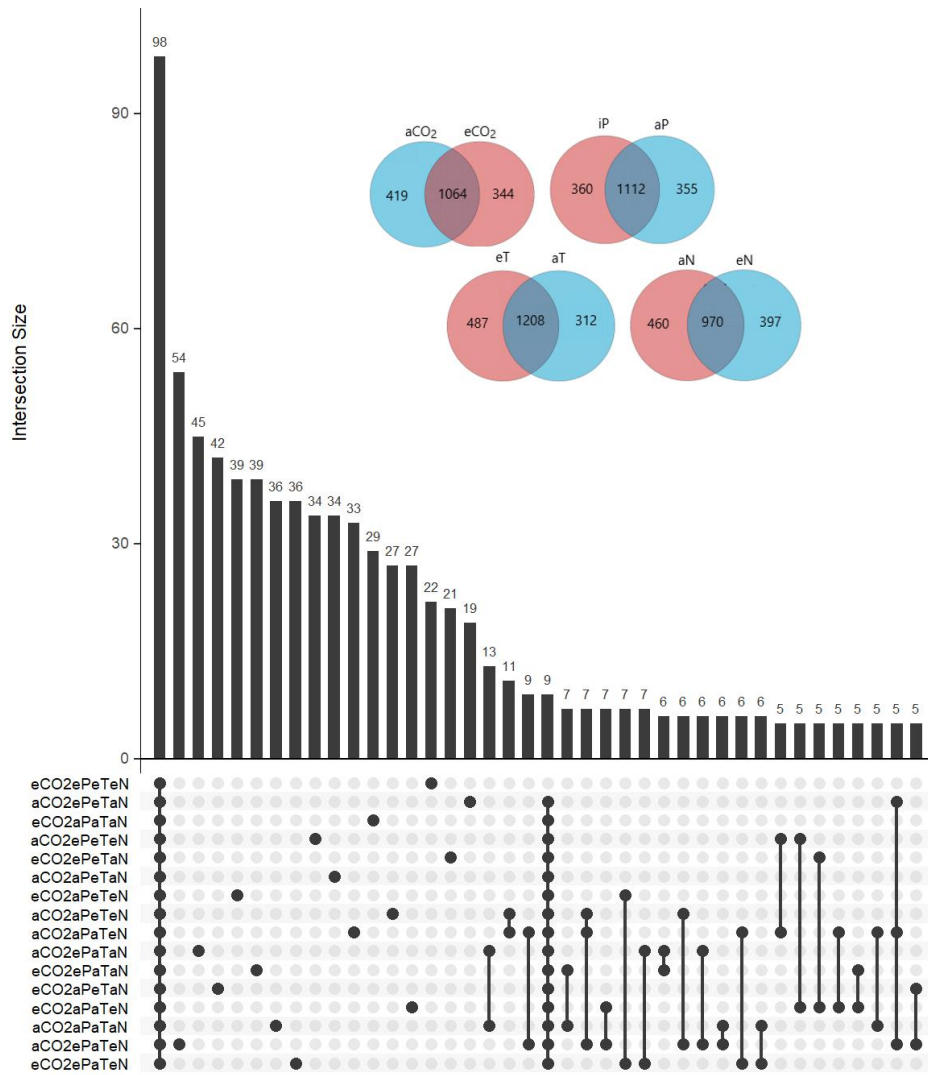


Fig. S3. Venn diagrams of detected AMF OTUs between ambient (a) and elevated (e) levels of the global change factors nitrogen (N), CO₂, temperature (T), and precipitation (P). Venn diagram detecting AMF specialist (unique) and generalist SVs (shared among treatments).

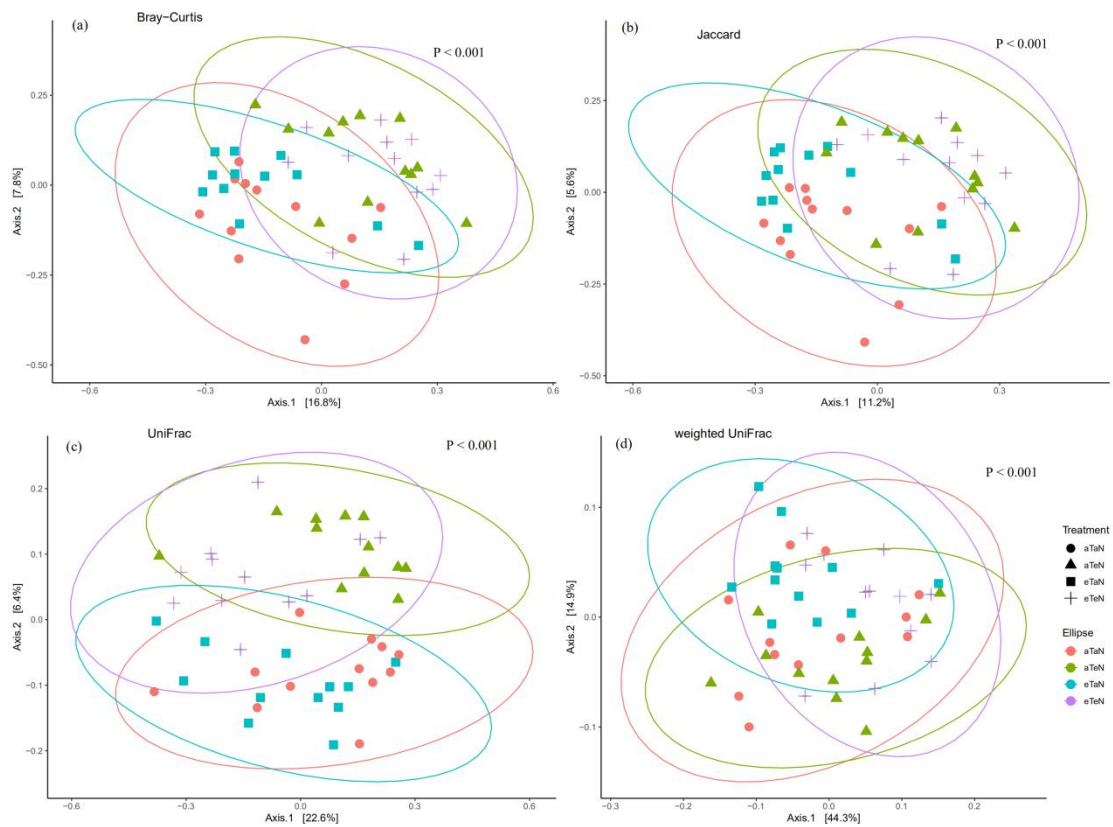


Fig. S4. Effects of nitrogen addition and elevated temperature on arbuscular mycorrhizal fungi community composition variation results from PCoA of Bray-Curtis distance (a), Jaccard distance (b), unweighted UniFrac distance (c), and weighted UniFrac distances (d).

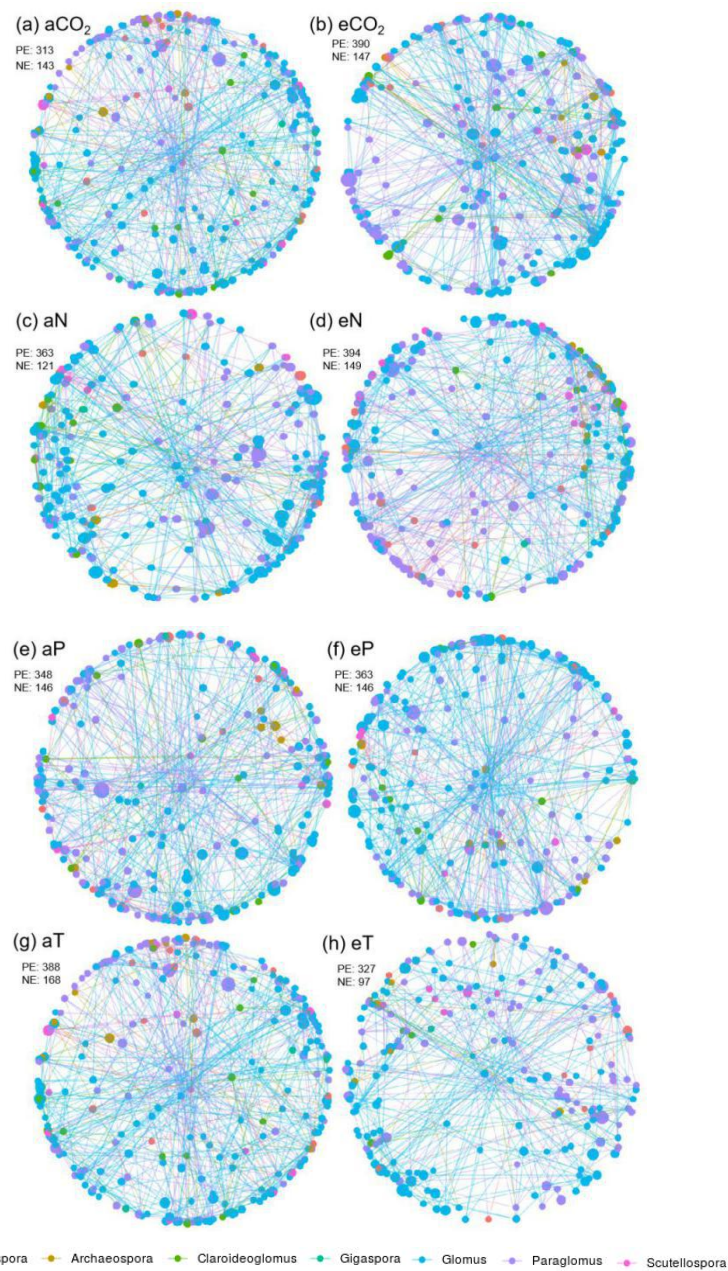


Fig. S5. Co-occurring network of AMF communities in soil samples from the ambient CO₂ (aCO₂) and elevated CO₂ (eCO₂), ambient N (aN) and enriched N deposition (eN), ambient precipitation (aP) and elevated precipitation (eP), and ambient temperature (aT) and elevated temperature (eT). Co-occurrence network was constructed with SPIEC-EASI. AMF OTU nodes were colored according to genus lineage. PE: Positive edge, NE: Negative edge, Positive and negative interactions indicate that the abundances of the OTUs changed following the same trend and the opposite trend across different soil samples, respectively.

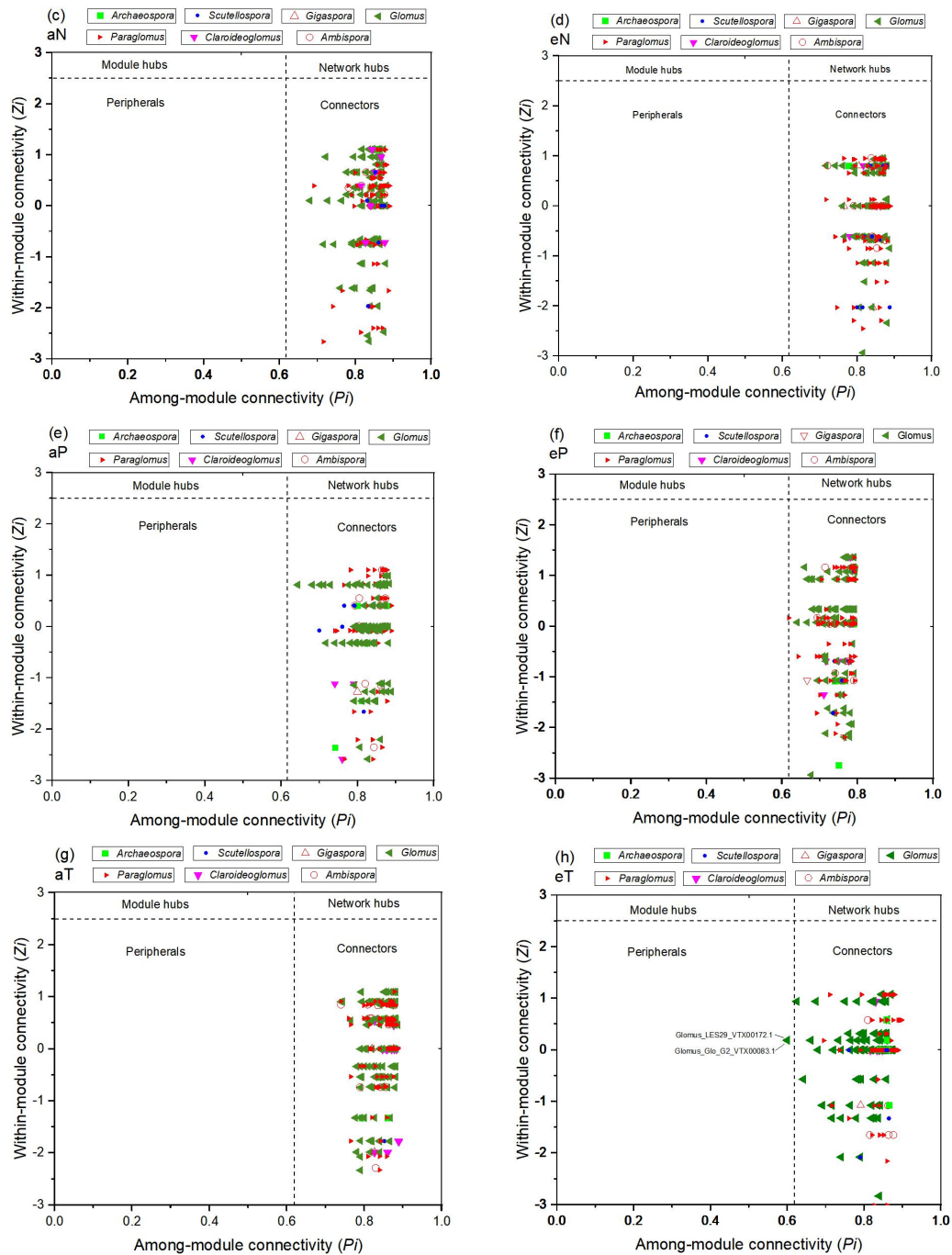


Fig. S6. Within (Z_i) and among-module (P_i) connectivity plots showing the distribution of AM fungi based on their topological roles. Each symbol represents an AM fungi OTU (or species). Different shapes of symbol indicate different genus. The topological roles of OTUs were determined according to the OTUs interconnecting in the same module (within-module connectivity) and in the different modules (among-module connectivity). The peripherals are labeled by OTUs identity numbers. Topological roles of interconnecting AM fungi OTUs in the same and different modules were calculated according to Olesen et al. (2007). The Horizontal and vertical dash lines represent the threshold value of Z_i (2.5) and P_i (0.62) to categorize OTUs, respectively.

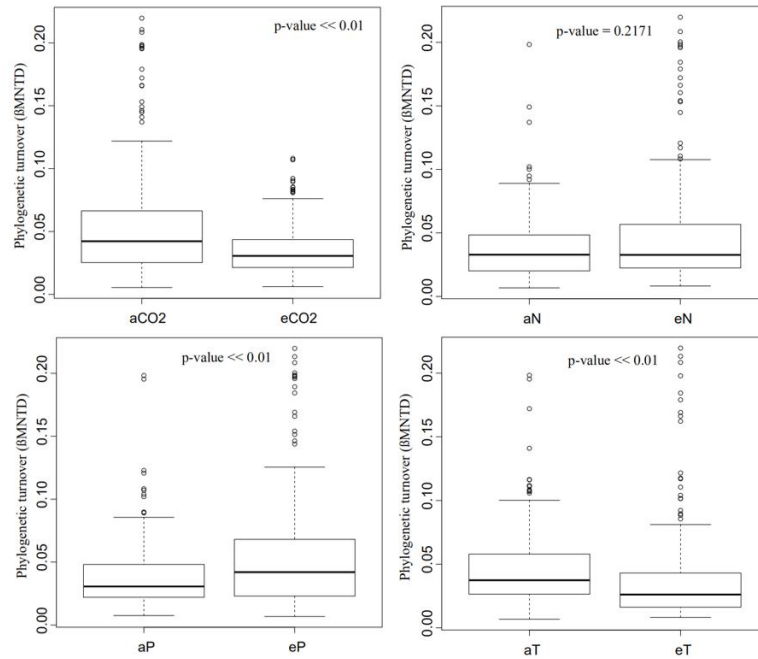
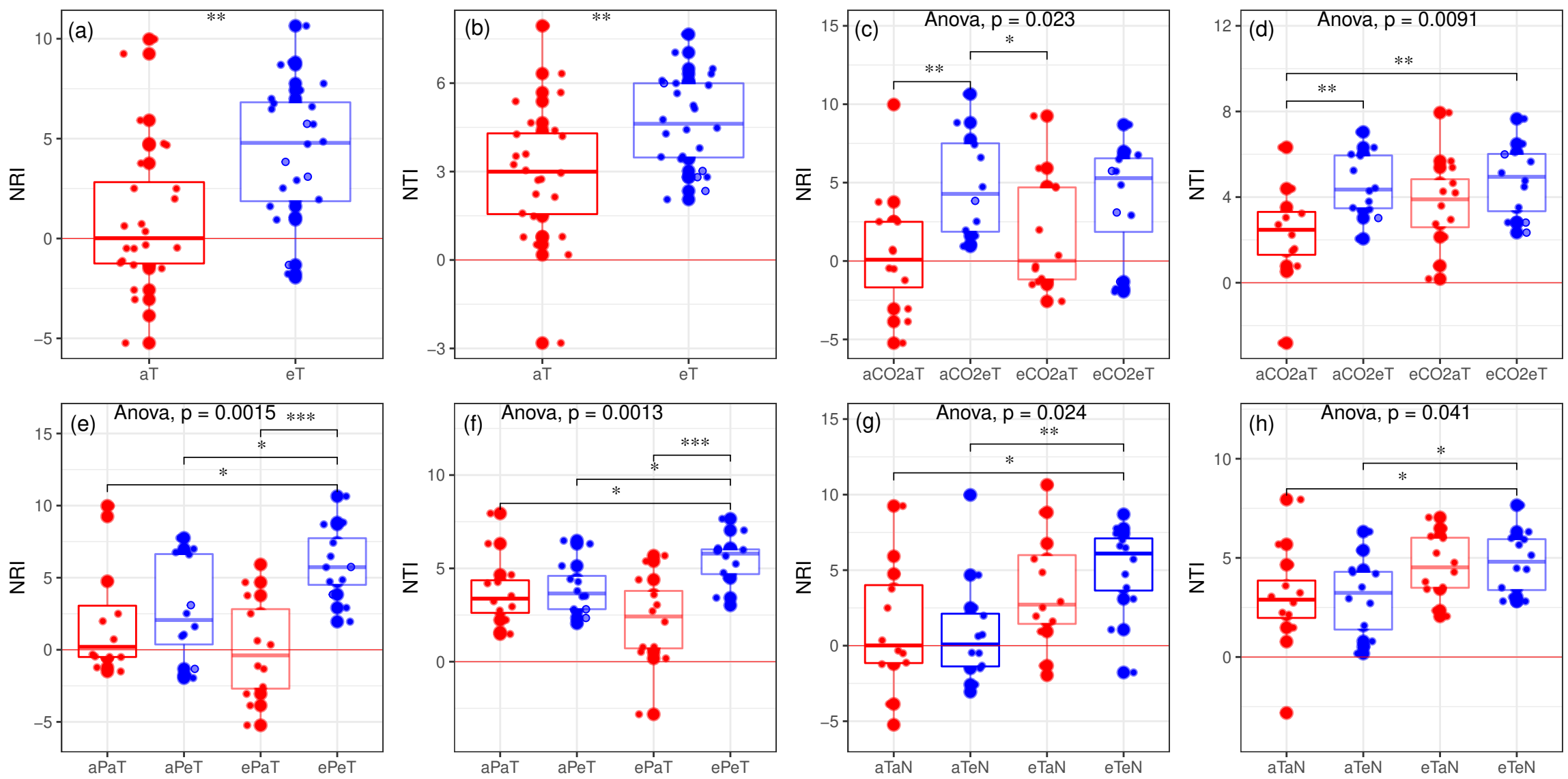


Fig. S7. Phylogenetic turnover of AMF communities under ambient CO₂ (aCO₂) and elevated CO₂ (eCO₂), ambient N (aN) and enriched N deposition (eN), ambient precipitation (aP) and elevated precipitation (eP), and ambient temperature (aT) and elevated temperature (eT) treatment. Line in the box represents median, the top and bottom of the box represents first and third quartiles, and the whisker represents 1.5 interquartile range. Wilcoxon test was used to detect the difference between ambient and elevated levels of GCFs.



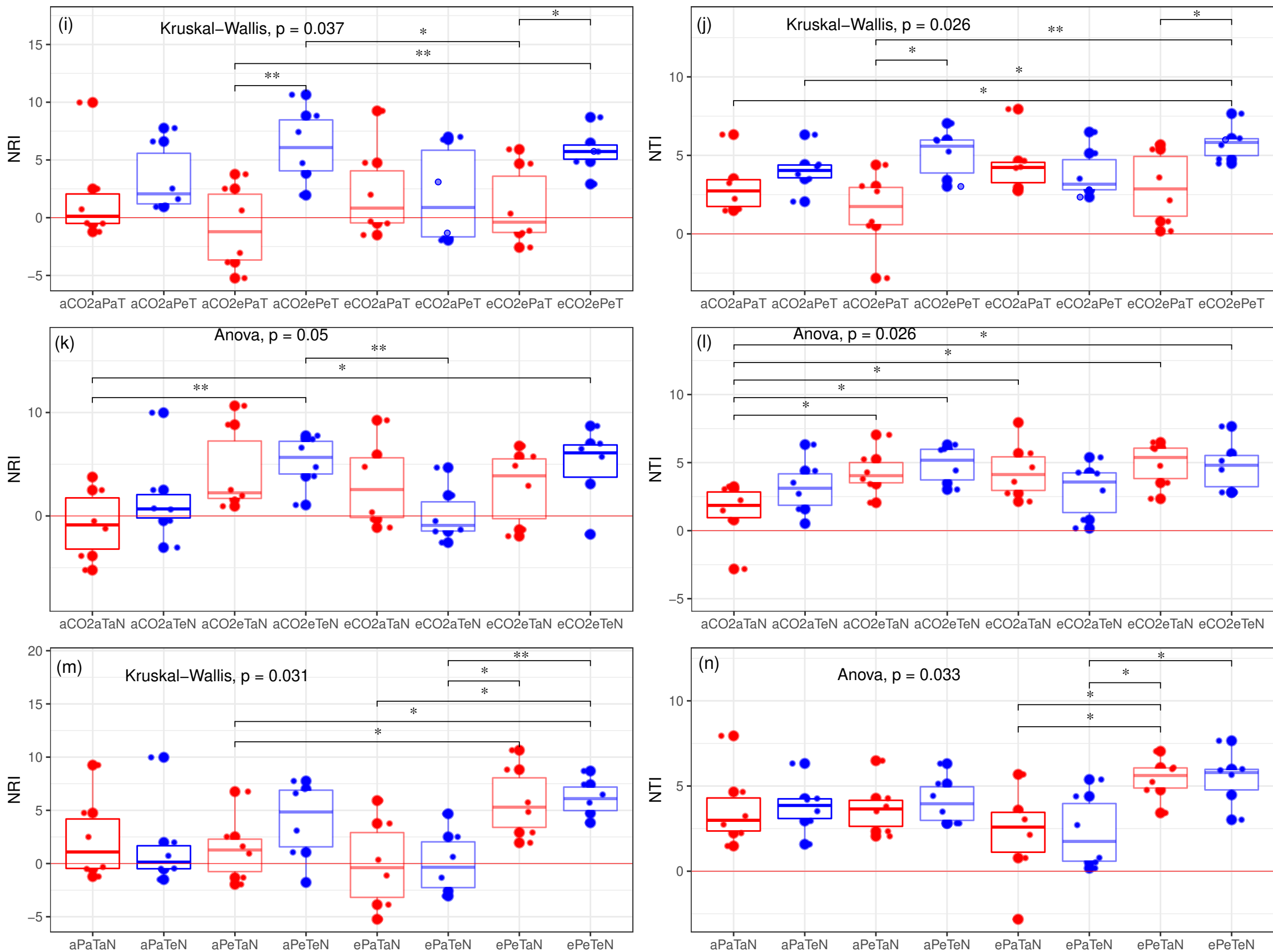


Fig.S8. Nearest related index (NRI) and nearest taxon index (NTI) of AMF community under GCFs treatments. Mean NRI and NTI that are significantly higher than zero, indicating phylogenetic clustering, lower than zero indicating overdispersal or phylogenetic evenness, and values close to zero indicating a phylogenetically random assembly of community.

Figures

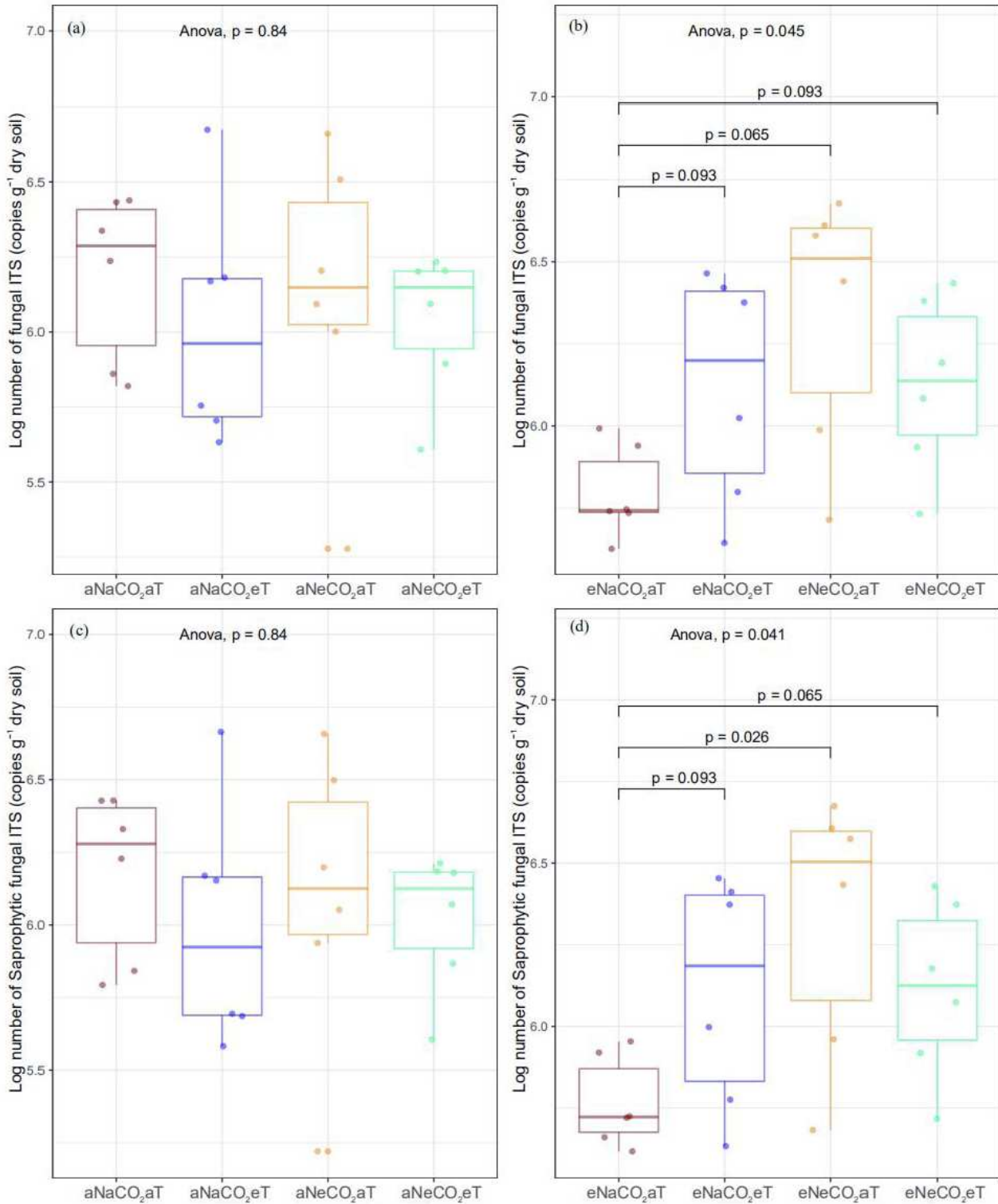


Figure 1

Three-way interaction effects of ambient (a) and elevated (e) levels of the global change factors nitrogen (N), CO₂, and temperature (T) on a, b total fungal biomass and c, d saprophytic fungal biomass (log number of ITS gene copies g⁻¹). The p-values above the lines are from Tukey's HSD post-hoc tests.

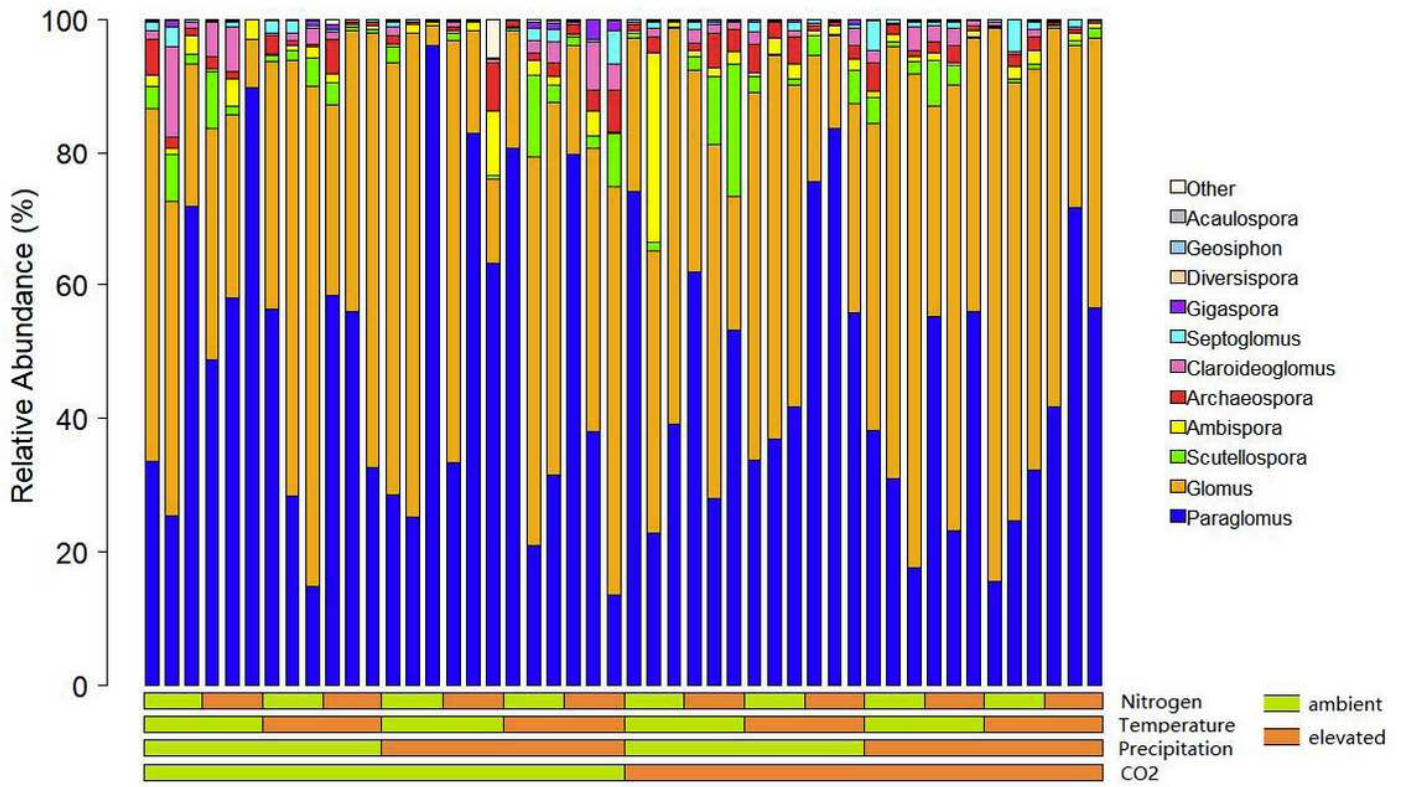


Figure 2

Relative abundances (%) of major genera of arbuscular mycorrhizal fungi under the influence of ambient and elevated levels of the global change factors nitrogen, CO₂, temperature, and precipitation.

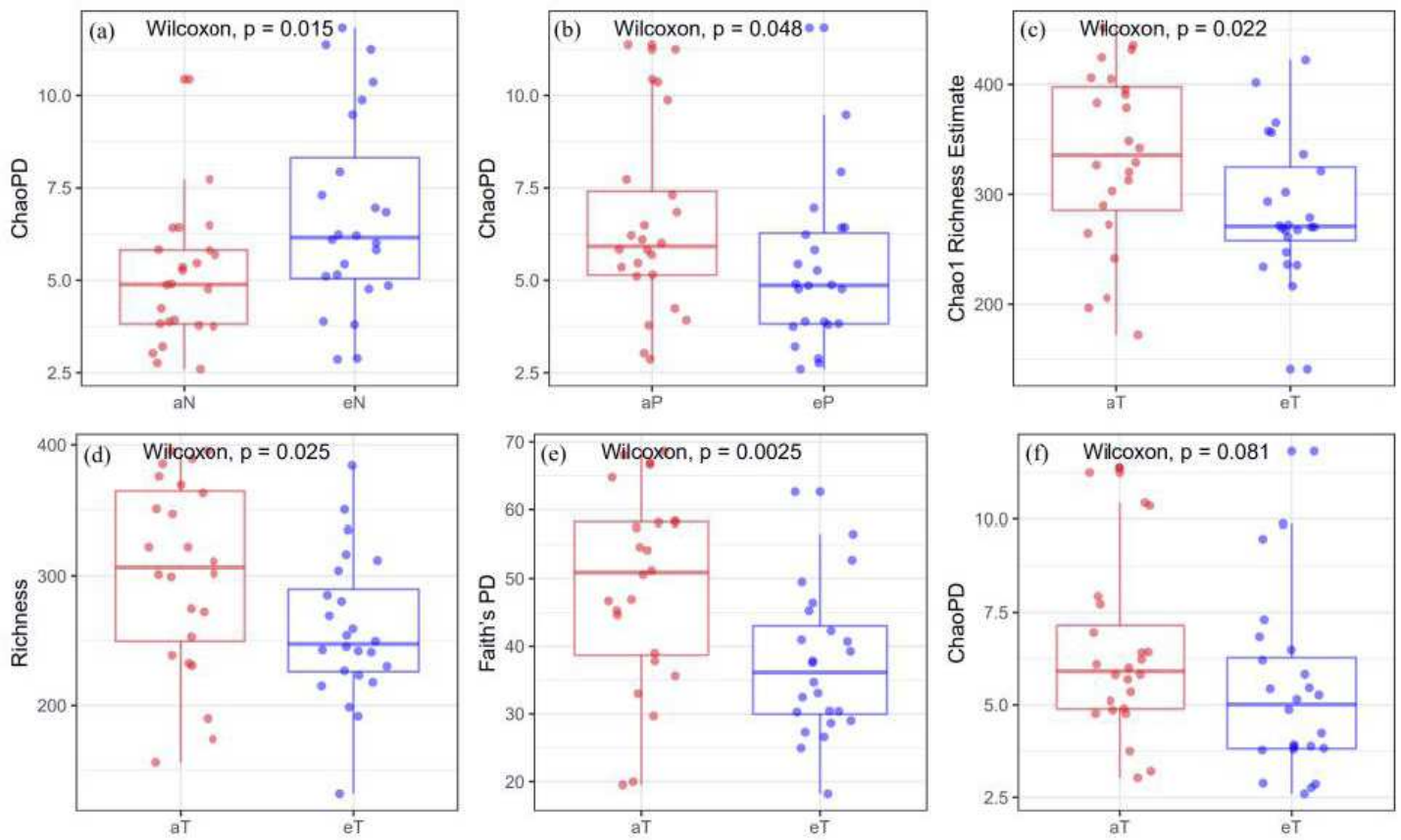


Figure 3

Significant effects of global change factors on arbuscular mycorrhizal communities. (a) Effect of nitrogen (N) addition on ChaoPD (phylogenetic diversity); (b) effect of elevated precipitation (P) on ChaoPD; and effect of elevated temperature (T) on (c) Chao1, (d) richness, (e) Faith's PD, and (f) ChaoPD. a, ambient level; e, elevated level.

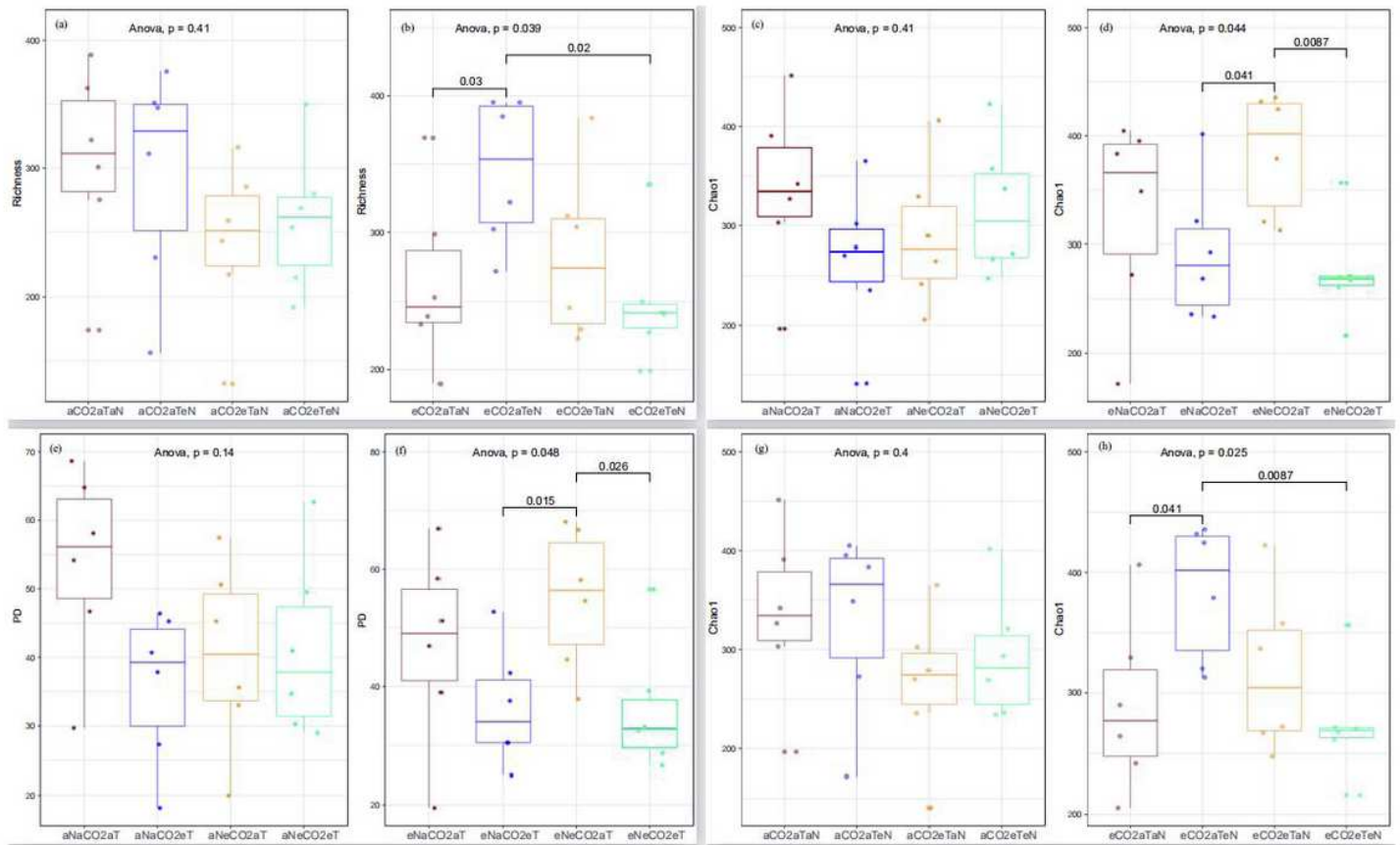


Figure 4

Three-way interaction effects of global change factors on arbuscular mycorrhizal fungal communities. a, b Effect of CO₂, nitrogen (N), and temperature (T) on richness; effect of N, CO₂ and T on c, d the Chao1 index and on e, f the phylogenetic diversity (PD) index; and g, h effect of CO₂, T, and N on the Chao1 index. Ambient (a) and elevated (e) levels.

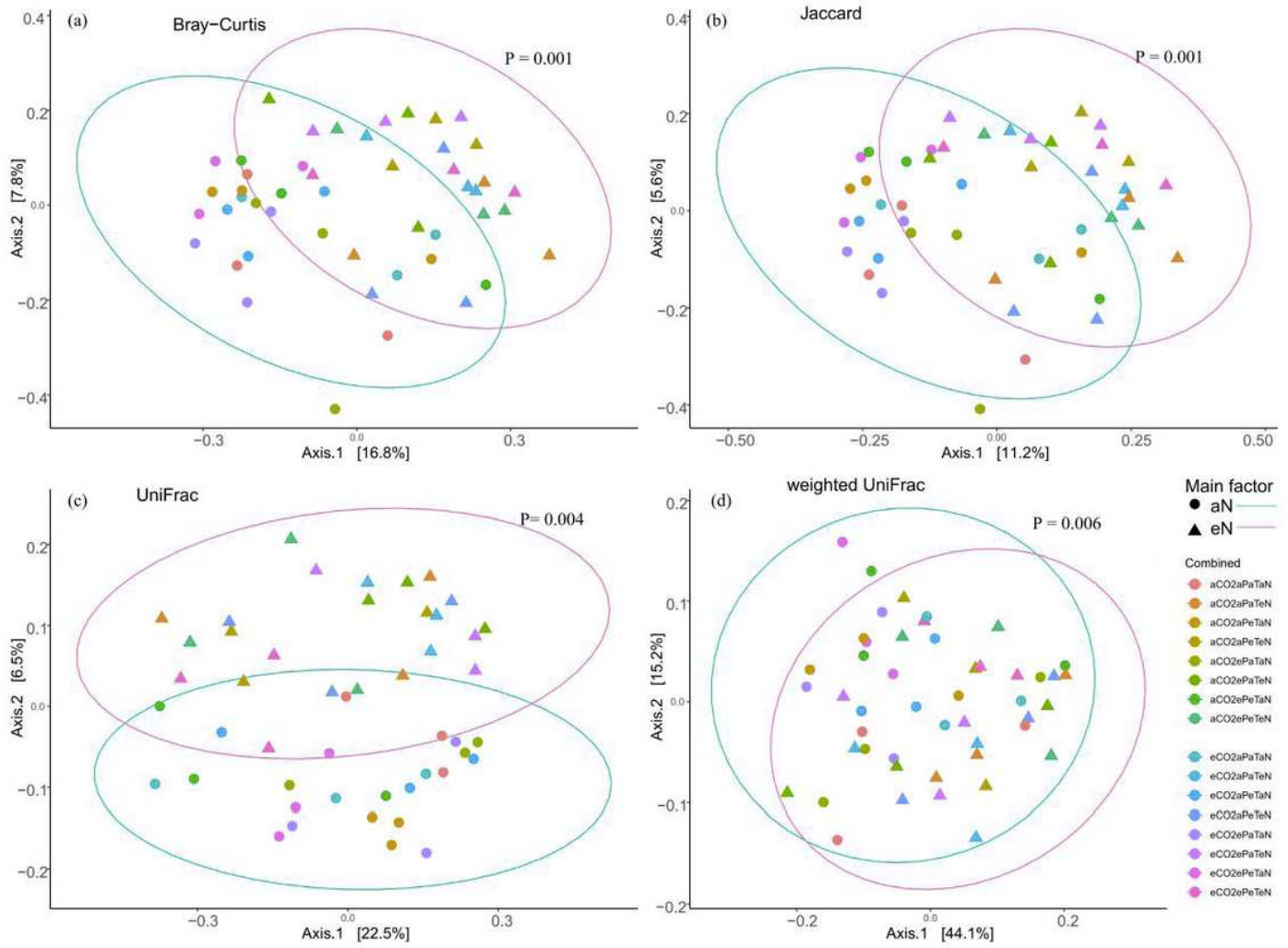


Figure 5

Principal coordinate analysis of the effects of nitrogen (N) addition on (a, ambient level; e, elevated level) on variation in arbuscular mycorrhizal fungal community composition. a Bray-Curtis distance, b Jaccard distance, c unweighted UniFrac distance, and d weighted UniFrac distances. P, precipitation; T, temperature.

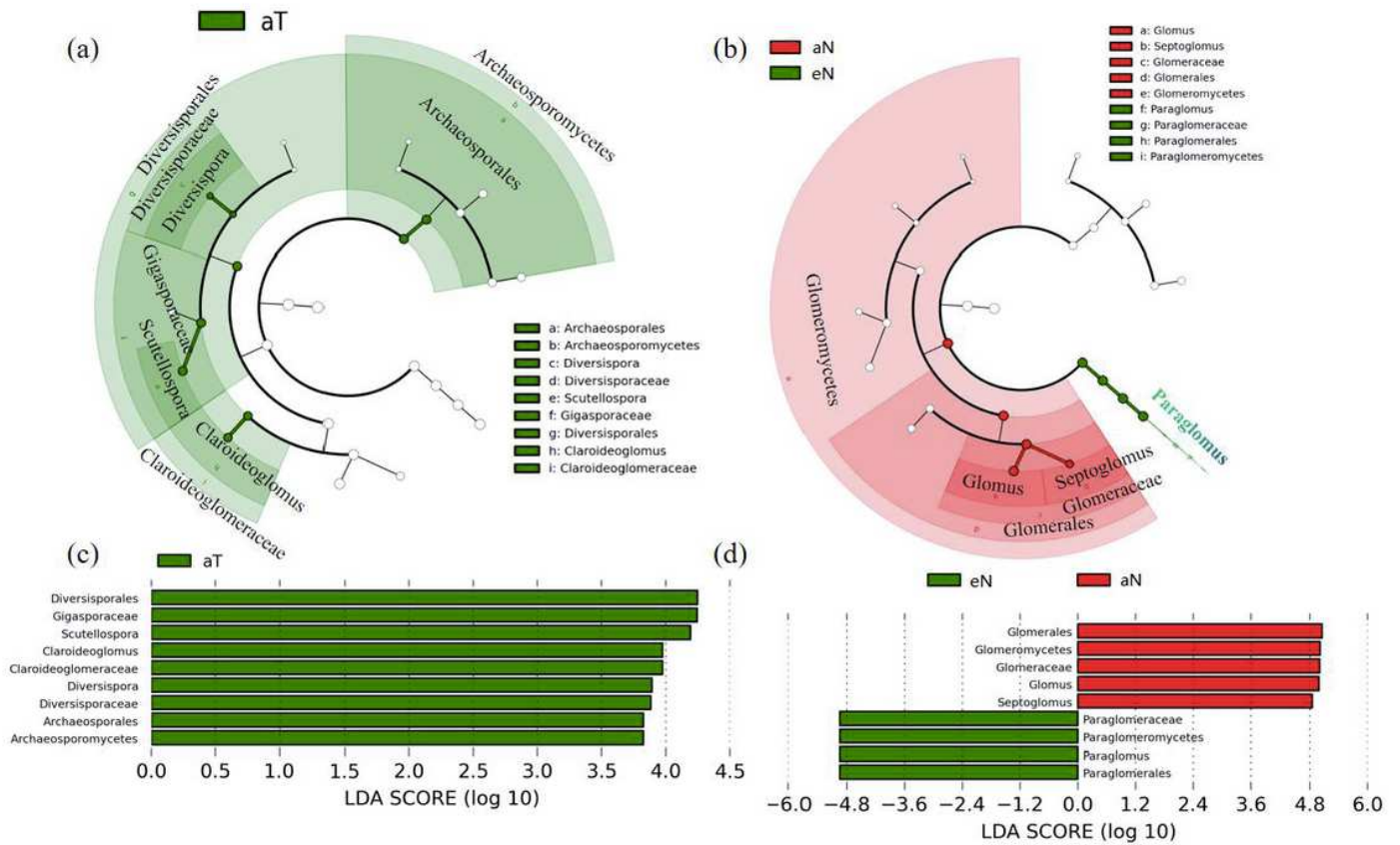


Figure 6

Discriminant taxa of arbuscular mycorrhizal fungal (AMF) communities as determined by LefSe analysis in a) warming and unwarmed treatment and b) fertilized and unfertilized treatment. AMF taxa are illustrated according to taxonomic relationships using a cladogram to show the discriminative patterns in taxonomic lineages. c) and d) AMF taxa listed according to linear discriminant analysis (LDA) values. Only the AMF lineages that showed significant responses to eCO₂, eN, eP and eT are shown (a, ambient level; e, elevated level; T, temperature; N, nitrogen; P, precipitation).

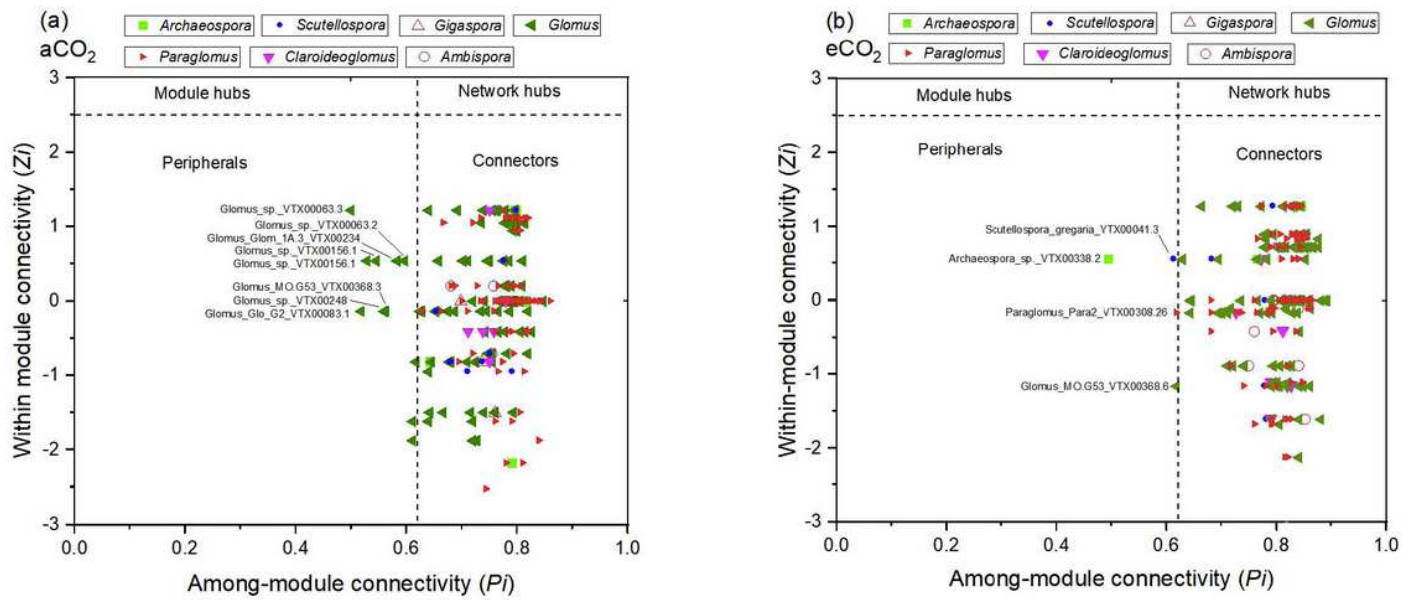


Figure 7

Within-module (Z_i) and among-module (P_i) connectivity plots showing the distribution of arbuscular mycorrhizal fungi (AMF) based on their topological roles under: a) ambient CO₂ (aCO₂), and b) elevated CO₂ (eCO₂). Each symbol represents an AMF operational taxonomic unit (OTU) (or species). Different symbols indicate different genera. The topological roles of OTUs were determined according to the OTUs interconnecting in the same module (within-module connectivity) and in different modules (among-module connectivity). The OTUs identity numbers label the peripherals. The horizontal and vertical dashed lines represent the threshold values of Z_i (2.5) and P_i (0.62), respectively, used to categorize OTUs.

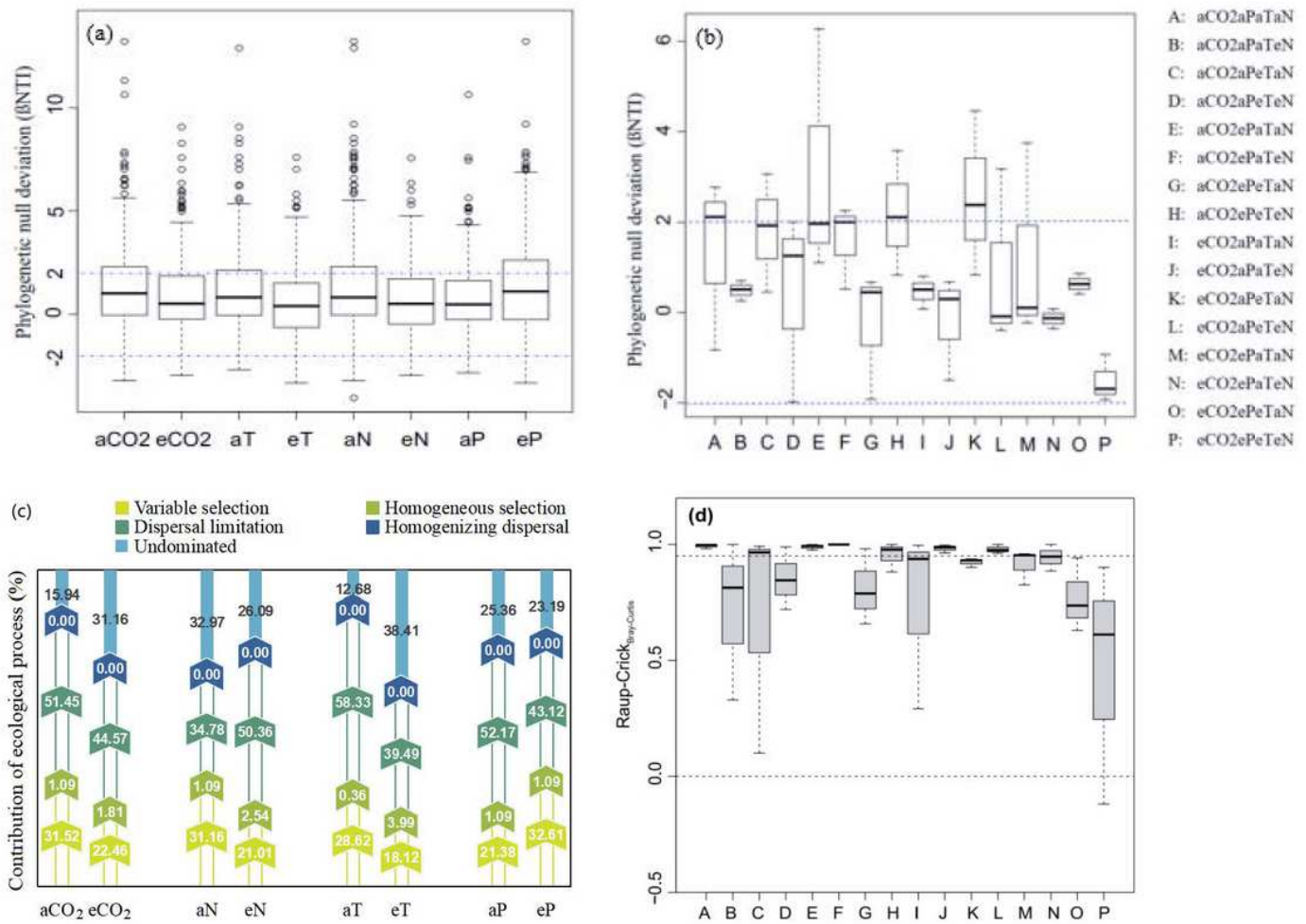


Figure 8

Ecological null model outputs (β NTI) of arbuscular mycorrhizal fungal (AMF) communities under a) the eight global change factor (GCF) treatments and under b) sixteen GCF treatments. In the box-and-whisker plots, the line in the box represents the median, the top and bottom of the box represent first and third quartiles, respectively, and the whiskers represent the 1.5 interquartile range. c) Contributions of community assembly processes governing AMF community turnover under the influence of GCFs. Ambient CO₂ (aCO₂), elevated CO₂ (eCO₂), ambient nitrogen (aN), elevated N (eN), ambient temperature (aT), elevated T (eT), ambient precipitation (aP), elevated P (eP). d) Raup-Crick_{Bray-Curtis} results for the AMF communities under sixteen GCF treatments.